

RESEARCH

Open Access



ZA-II-05, a novel NMDA-receptor antagonist reverses vanadium-induced neurotoxicity in *Caenorhabditis elegans* (*C. elegans*)

Amany Ladagu¹, Funmilayo Olopade², Paul Chazot³, Taiwo Elufioye⁴, Toan Luong⁵, Madison Fuller⁵, Ethan Halprin⁶, Jessica Mckay⁶, Zeynep Ates-Alagoz⁷, Taidinda Gilbert¹, Adeboye Adejare^{6*} and James Olopade¹

Abstract

Introduction Vanadium is a widely used transition metal in industrial applications, but it also poses significant neurotoxic and environmental risks. Previous studies have shown that exposure to vanadium may lead to neurodegenerative diseases and neuropathic pain, raising concerns about its impact on human health and the ecosystem. To address vanadium neurotoxicity, through targeting NMDA glutamate and dopamine signaling, both involved in neurodegenerative disorders, shows promise. Using *Caenorhabditis elegans* as a model, we evaluated a novel compound with a mixed NMDA glutamate receptor-dopamine transporter pharmacology, ZA-II-05 and found it effectively ameliorated vanadium-induced neurotoxicity, suggesting a potential neuroprotective role.

Methods Synchronized young adult worms were assigned to four different experimental groups; Controls; 100 mM of Vanadium; Vanadium and 1 mg/ml ZA-II-05; and ZA-II-05 alone. These were examined with different markers, including DAPI, MitoTracker Green and MitoSox stains for assessment of nuclei and mitochondrial density and oxidative stress, respectively.

Results Exposure to vanadium in *C. elegans* resulted in decreased nuclear presence and reduction in mitochondrial content were also analyzed based on fluorescence in the pharyngeal region, signifying an increase in the production of reactive oxygen species, while vanadium co-treatment with ZA-II-05 caused a significant increase in nuclear presence and mitochondrial content.

Discussion Treatment with ZA-II-05 significantly preserved cellular integrity, exhibiting a reversal of the detrimental effects induced by vanadium by modulating and preserving the normal function of chemosensory neurons and downstream signaling pathways. This study provides valuable insights into the mechanisms of vanadium-induced neurotoxicity and offers perspectives for developing therapeutic interventions for neurodegenerative diseases related to environmental toxins.

Keywords Vanadium, Neurodegenerative diseases, NMDA receptor antagonist, Neurotoxicity, *Caenorhabditis elegans*

*Correspondence:

Adeboye Adejare
aadejare@sju.edu

Full list of author information is available at the end of the article



© The Author(s) 2024. **Open Access** This article is licensed under a Creative Commons Attribution-NonCommercial-NoDerivatives 4.0 International License, which permits any non-commercial use, sharing, distribution and reproduction in any medium or format, as long as you give appropriate credit to the original author(s) and the source, provide a link to the Creative Commons licence, and indicate if you modified the licensed material. You do not have permission under this licence to share adapted material derived from this article or parts of it. The images or other third party material in this article are included in the article's Creative Commons licence, unless indicated otherwise in a credit line to the material. If material is not included in the article's Creative Commons licence and your intended use is not permitted by statutory regulation or exceeds the permitted use, you will need to obtain permission directly from the copyright holder. To view a copy of this licence, visit <http://creativecommons.org/licenses/by-nc-nd/4.0/>.

Introduction

Vanadium, a transition metal widely used in industrial applications, has garnered attention for its neurotoxic and environmentally hazardous properties. Its increasing presence in the environment poses a persistent threat to both human health and the ecosystem [1]. Accumulating evidence using animal models suggests that exposure to vanadium can lead to neurodegenerative diseases, including Alzheimer's disease (AD) and Parkinson's disease (PD), [2, 3] as well as neuropathic pain, raising concerns about the potential impact on neurological functions [4–6]. Vanadium can penetrate the blood–brain barrier, allowing direct access to neural tissues. Once inside the brain, it has been linked to various detrimental effects, such as cognitive deficits, neuronal damage, and disruption of the blood–brain barrier integrity [7, 8]. Additionally, the association between vanadium neurotoxicity and the pathogenesis of neurodegenerative diseases highlights the urgency to explore effective therapeutic approaches for mitigating its harmful impact. One promising avenue for addressing vanadium neurotoxicity lies in targeting NMDA receptors, a subtype of glutamate receptors and dopamine transmission. These receptors have been implicated in various neurodegenerative disorders, and modulating their activity with specific antagonists has demonstrated efficacy against excitotoxicity, a key mechanism underlying neural damage in several neurodegenerative conditions [9–11].

ZA-II-05 (Fig. 1) is a compound initially designed as an NMDA receptor antagonist but also exhibits affinity for other neurotransmitter receptors like dopamine transporter, opioid receptors, and sigma receptors [11]. This versatility, known as “off-target” binding, arises from structural similarities among receptors. In binding assays, ZA-II-05 showed significant affinity for dopamine transporter, opioid receptors, and sigma receptors, with K_i values ranging from 5.5 nM to 3161 nM. It also moderately bound to GluN1/GluN2A and GluN1/GluN2B subtype receptors. These characteristics position ZA-II-05 as a promising candidate for treating neuropsychiatric

disorders, especially those related to NMDA receptor dysfunction or neurotoxicity [9, 11]. In studies on vanadium-induced neurotoxicity using mice, ZA-II-05 displayed considerable protection against neuronal damage. Moreover, in preclinical trials assessing maximal electroshock seizures, ZA-II-05 demonstrated anticonvulsant properties at doses of 100 and 300 mg/kg (i.p.), suggesting potential for managing seizures while preserving normal neurological functions. With rigorous safety testing and NIH approval for animal experimentation, ZA-II-05 emerges as a versatile therapeutic agent for various neurological and neuropsychiatric conditions [11].

To investigate the potential neuroprotective effect of ZA-II-05 on vanadium-induced neurotoxicity, the nematode *Caenorhabditis elegans* (*C. elegans*) serves as an ideal model system. This transparent, genetically tractable organism offers unique advantages for studying neurotoxicity and neuroprotection due to its well-characterized nervous system and rapid lifecycle [12, 13]. The neuronal system of *C. elegans* consists of 302 neurons, organized into sensory, motor, and interneurons, controlling the worm's behavior and movement [14]. The nervous system includes a nerve ring (the brain) and ventral and dorsal nerve cords, which regulate movement [15]. *Caenorhabditis elegans* communicate using neurotransmitters such as acetylcholine, GABA, glutamate, dopamine, and serotonin [16]. Despite its simplicity, the nervous system exhibits plasticity, allowing the worm to respond to environmental stimuli [17]. The fully mapped synaptic connections, or connectome, make *C. elegans* a valuable model for neurobiology, particularly in studying molecular and cellular mechanisms underlying neurotoxicity and neurodegeneration [18]. Neurons in *C. elegans* are categorized into 118 classes based on function, location, and connectivity [19]. Key examples include mechanosensory neurons (PLM, AVM, PVD) responsible for touch sensitivity, interneurons (AIB, RIA, RIM) involved in information processing and movement coordination, and D-type motor neurons controlling body wall muscles

Compound	Molecular Formula
ZA-II-05	C ₂₅ H ₃₄ FNO ₆

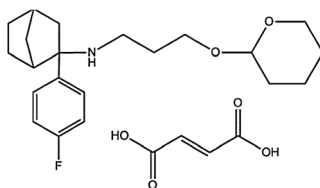


Fig. 1 ZA-II-05; novel uncompetitive NMDA-receptor antagonist. IUPAC name_2-(4-fluorophenyl)-N-(3-[(tetrahydro-2H-pyran-2-yl)oxy]propyl)bicyclo [2.2.1] heptan-2-amine

[20]. The mitochondria, as well, play a crucial role in cellular function, are highly vulnerable to oxidative stress and are considered the primary source of reactive oxygen species (ROS) production [21, 22]. Researchers have also identified several types of glutamate receptors in this organism. These include: mGluRs, GluCl and iGluRs (ionotropic glutamate receptors), iGluRs function as glutamate-gated ion channels, multiple glutamate receptor subunits have been identified, forming heteromeric glutamate-gated cation channels. These include two NMDA-type receptors (NMR-1 and NMR-2) and eight non-NMDA-type receptors (GLR-1 to GLR-8). Unlike NMDA receptors, which are involved in long-term potentiation and synaptic plasticity in mammals, these iGluRs in *C. elegans* primarily mediate fast excitatory neurotransmission [23, 24].

In *C. elegans*, DAT-1, the dopamine transporter, controls the levels of extracellular dopamine (DA) at synapses, thus modulating synaptic dopamine signaling [25]. The DAT-1 protein is responsible for reuptake of dopamine from the synaptic cleft into presynaptic neurons, thereby terminating the action of dopamine at synapses [26]. This is similar to the function of the dopamine transporter in mammals. Dopamine signaling, found in both vertebrates and invertebrates, plays a role in memory, motivation, hormonal regulation, rewards, recognition, motor control and adaptive responses. In humans, disruptions in dopamine signaling are linked to numerous neurological disorders such as Alzheimer's disease, Parkinson's disease, and attention deficit hyperactivity disorder (ADHD) [27, 28]. In *C. elegans*, dopamine signaling shares many key molecular components with mammalian systems [29]. Studies using *C. elegans* have identified a wide range of compounds with neurotoxic effects, including heavy metals (e.g., vanadium, lead, mercury, cadmium), pesticides, industrial chemicals, and environmental pollutants (e.g., polychlorinated biphenyls, polycyclic aromatic hydrocarbons) [30, 31]. These toxicants can induce neuronal degeneration, oxidative stress, mitochondrial dysfunction, and disruptions in neurotransmitter signaling pathways [32, 33]. Research in *C. elegans* has also elucidated various molecular and cellular mechanisms underlying neurotoxicity, including excitotoxicity, oxidative stress, mitochondrial dysfunction, protein aggregation, and inflammation [34, 35]. These studies have identified conserved genetic pathways and molecular targets implicated in neurodegenerative diseases in humans [36, 37]. *Caenorhabditis elegans* has been instrumental in screening for neuroprotective compounds and elucidating mechanisms of neuroprotection against neurotoxic insults. Compounds like ZA-II-05 with antioxidant, anti-inflammatory, and chelating properties [9, 11] show promise in mitigating neurotoxicity

and preserving neuronal function in *C. elegans* models of neurodegeneration.

In this study, we aimed at exploring the efficacy of a novel mixed NMDA receptor-dopamine transporter antagonist-inhibitor, ZA-II-05, a multi-targeted directed ligand (MTDL), in ameliorating vanadium-induced neurotoxicity in *C. elegans*. MTDLs are a type of drug or compound designed to simultaneously interact with multiple biological targets, rather than just a single target, in order to achieve a therapeutic effect [38, 39]. This approach contrasts with the traditional "one drug, one target" model and is particularly relevant in treating complex diseases, such as neurodegenerative disorders, cancer, and cardiovascular diseases, where multiple pathways are involved [40, 41]. For example, in neurodegenerative diseases like Alzheimer's, which involve multiple pathways such as amyloid-beta aggregation, tau protein dysfunction, oxidative stress, and cholinergic deficit, an MTDL could simultaneously address several of these issues [42, 43]. The design of MTDLs can involve combining pharmacophores (the parts of a molecule that interact with biological targets) into a single compound or developing hybrid molecules that possess the activity of more than one drug [44]. In essence, MTDLs represent a modern approach to drug discovery and development that aligns with the understanding that many diseases involve multiple interconnected pathways, requiring a more holistic therapeutic strategy.

By leveraging the transparency and genetic manipulation capabilities of this model organism, we can gain valuable insights into the mechanisms underlying vanadium neurotoxicity and the potential therapeutic benefits of NMDA receptor-dopamine modulation [11]. The findings from this research (Fig. 2) may pave the way for the development of novel strategies for mitigating the neurotoxic effects of vanadium exposure, offering hope for future therapeutic interventions in the prevention and treatment of neurodegenerative diseases related to environmental toxin exposure.

Materials and methods

Chemicals

Sodium metavanadate (NaVO_3) (Sigma, St. Louis, MO, USA) was utilized in this study. Novel NMDA-receptor antagonist ZA-II-05, a bicyclic aryl cyclohexylamine, was designed and synthesized in our lab. Several tests established safety of the compound at dosages envisioned in this study.

Synthesis of the ZA-II-05

ZA-II-05 (2-[4-Fluorophenyl]-N-(3-[tetrahydro-2H-pyran-2-yloxy] propyl) bicyclo [2.2.1] heptan-2-amine) was synthesized as the fumarate salt (1:1) in our

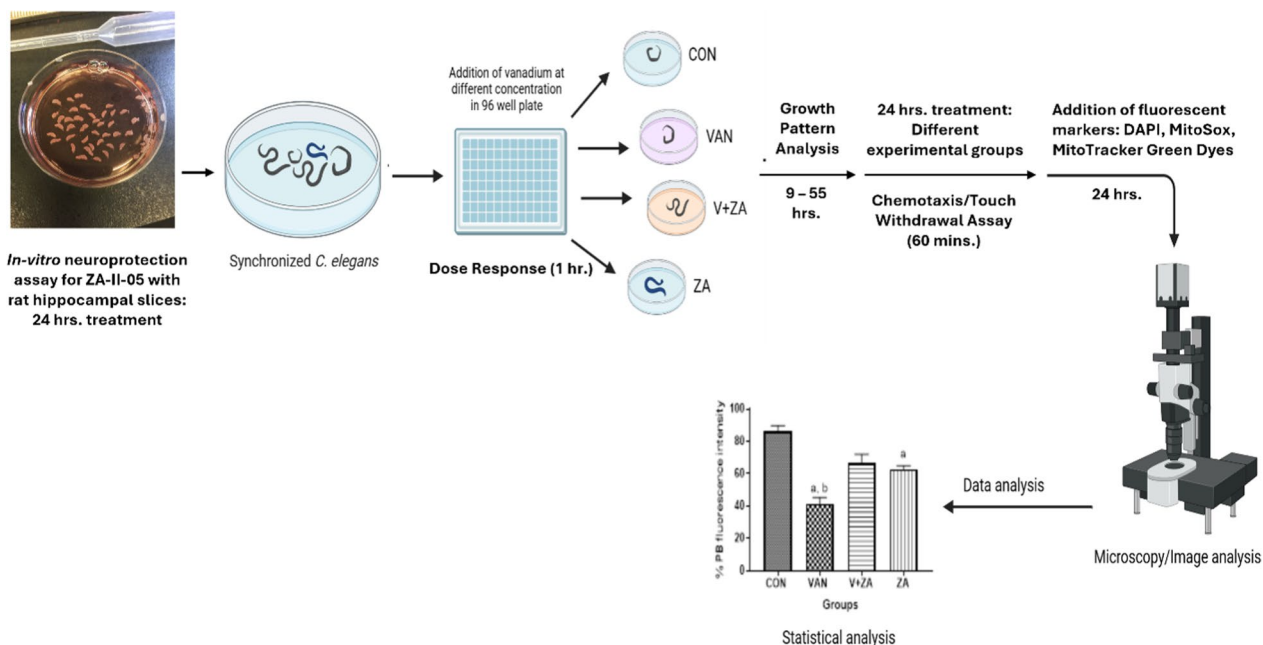


Fig. 2 Schematic diagram depicting the timeline of treatments and assays. CON-Control, VAN-Vanadium, V+ZA-Vanadium+ZA-II-05, ZA-ZA-II-05

laboratory as a colorless crystalline compound, m.p. 163–165 °C [45]. The structure was confirmed by NMR and MS techniques.

^1H NMR (400 MHz, CDCl_3) d ppm 7.37–7.26 (m, 2H), 7.06–6.95 (m, 2H), 4.51 (s, 1H), 3.80 (s, 1H), 3.70 (s, 1H), 3.48 (d, $J=5.53$ Hz, 1H), 3.37 (d, $J=6.11$ Hz, 1H), 2.45 (s, 1H), 2.35 (s, 1H), 2.32–2.21 (m, 1H), 2.21–2.11 (m, 1H), 2.11–2.03 (m, 1H), 1.81 (dd, $J=19.13$ Hz, 3H), 1.67 (s, 1H), 1.64–1.43 (m, 7H), 1.43–1.26 (m, 3H), 1.03 (d, $J=6.97$ Hz, 2H); ^{13}C NMR (400 MHz, CDCl_3) d ppm; 162.30, 159.97, 140.34, 129.22, 114.24, 98.47, 67.74, 66.19, 62.19, 46.79, 46.56, 41.89, 41.62, 37.09, 36.00, 30.71, 30.56, 29.15, 25.49, 24.37, 19.62; ^{19}F (400 MHz, CDCl_3) d ppm -117.64; MS (ESI+) m/z: 348 (100%), $[\text{M}+\text{H}]$.

ZA-II-05 primary screen for neuroprotection

Primary screen experiment according to methods previously done [46], was carried out as a qualitative assessment of the ability of ZA-II-05 to prevent excitotoxic cell death. This assay offers a powerful and versatile approach for understanding drug effects on brain function, providing critical insights into both neurotoxicity and therapeutic potential in the drug discovery process [47, 48]. Organotypic hippocampal slice cultures were treated with *N*-methyl-*D*-aspartate (NMDA) at 10 μM to induce neuronal cell death. The hippocampus is particularly vulnerable to neurotoxic insults, including excitotoxicity (e.g., from excessive glutamate receptor

activation), oxidative stress, and metal toxicity such as lead and vanadium [11]. Hippocampal slices allow for in-depth investigation of the specific anatomical effects of toxicants on neuronal health, including synaptic connections and degeneration, dendritic damage, and cell death [49]. Propidium iodide (PI), a membrane-impermeant compound, was included in all wells of the culture plate. Dying cells have compromised cell membranes, thus PI in-vitro preliminary studies using hippocampal slice culture neuroprotection assay (NP) may diffuse into the cell, intercalate with DNA and fluoresce. The intensity of the PI fluorescence is proportional to the amount of cell death in the individual slices. Hippocampal slice cultures were treated with the excitotoxin, NMDA (10 μM) alone, and with the excitotoxin, NMDA and ZA-II-05 at the concentrations indicated (10 μM , 10 mM, 100 μM and 100 mM). After the experimental incubation period, the media was replaced with normal culture media containing PI, and images were captured again after an additional 24 h (t24). Media containing 50 mM glutamate was added and incubated for 1 h, then removed, and slices were re-imaged after 24 h in normal culture media with PI (tGLUT) to induce maximal staining intensity in each slice. Relative intensity ratios were calculated for each slice using the following equation: $(t24-t0)/(t\text{GLUT}-t0)$. Cell death was assessed by quantifying the uptake of 2 μM propidium iodide, with fluorescence intensity measured using an EVOS FL digital inverted microscope equipped with a Texas Red filter. The settings included

80% transmittance, a 1.0 s exposure, and 4× magnification. Statistical analysis was conducted using one-way ANOVA to evaluate significant differences in propidium iodide uptake between the experimental groups with GraphPad Prism 7.0. All analyzed groups consisted of a random sample size of 15–18 slices collected from 2–3 different litters of rat pups. Slice images were evaluated for staining intensity at each time point using NIH Image J software.

Strain growth, maintenance, and synchronization

The Bristol N2 (WT) strain of worms was employed for this study. The animals were cultured on standard NGM agar plates with OP50 *E. coli* as food, bacteria at a temperature range of 15–20 °C. To ensure synchronized growth, eggs were obtained by hatching overnight after treatment with sodium hypochlorite bleach, following the protocols previously outlined [50]. Subsequently, approximately 200–250 worms were transferred onto NGM agar plates seeded with OP50 and allowed to grow until reaching adulthood.

Dose response assay

The dose response of vanadium was carried out to determine the effects of its various concentrations on the worms. This assay helped in identifying the dose-dependent relationship between vanadium and its biological impact on the worms. It established the toxic threshold of vanadium, to evaluate its potential side effects in a controlled and measurable manner. 5000 synchronized L1 N2 worms were exposed to acute treatment in M9 buffer for 1 h in siliconized tubes with varying concentrations of vanadium, namely 5, 10, 50, 100, 150, and 200 mM, and a Control group without vanadium following the procedures previously outlined [13, 22, 51]. The tubes with the treated worms were centrifuged at 7000 rpm for 2 min and rinsed four times with 85 mM NaCl. Afterward, worms were plated in triplicates onto OP50-seeded NGM plates. Forty-eight hours after treatment, the total number of worms that survived was assessed as a percentage of the initial worm count that were used. The experiment was repeated six times using independent worm preparations, and the dose of vanadium that exhibited toxicity without causing total lethality was determined.

Growth pattern measurement

Growth patterns reflect the overall health and developmental progress of *C. elegans*. Inhibition of growth is a common endpoint in toxicity studies and can help evaluate the efficacy of potential therapeutics in drug discovery [52, 53]. Growth pattern assessment was carried out according to methods previously done [54]. Synchronized eggs were placed on NGM plates coated with OP50

E. coli bacteria, pre-treated ZA-II-05 and vanadium corresponding to the different experimental groups: Control group, 100 mM Vanadium, 1 mg/ml ZA-II-05, and a ZA-II-05-only group, with all treatments dissolved in sterile water or M9 buffer. The plates were incubated at 20 °C. Worm body length and survival were monitored at specific developmental stages based on the typical life cycle of wild-type *C. elegans* at 20 °C: 9 h (L1 larvae), 21 h (L2 larvae), 29 h (L3 larvae), 37 h (L4 larvae), 47 h (young adult), and 55 h (mature adult) post-egg laying [55]. Worm images were captured using an Evos FL digital inverted microscope and analyzed for body length using ImageJ software (<http://rsbweb.nih.gov/ij/>, National Institutes of Health, USA). The tests were independently repeated 3–5 times, with approximately 20–30 worms scored in each experiment.

Assessment of mitochondrial density and membrane potential

To evaluate the overall health and functionality of mitochondria, assessment of mitochondrial density and membrane potential were carried out. Mitochondrial density provides insights into changes in the number of mitochondria, which can reflect cellular energy needs or mitochondrial biogenesis. Membrane potential is a key indicator of mitochondrial functionality, as it reflects the ability of mitochondria to produce ATP and maintain ionic balance [56]. Changes in mitochondrial density and membrane potential was used to assess the impact of vanadium on mitochondrial health and to evaluate the effectiveness of potential therapeutic interventions of ZA-II-05 in restoring normal mitochondrial function.

Briefly, synchronized adult worms belonging to different experimental groups comprising of 2500 worms per group (Control group; 100 mM of Vanadium, and 1 mg/ml of ZA-II-05; and ZA-II-05 only, all dissolved in sterile water or M9 buffer) were incubated at a temperature of 20 °C for 24 h. 1 mg/ml (2 μM) of ZA-II-05 was used for the treatment of worms based on preliminary data obtained (Unpublished) and previous studies with memantine, an NMDA receptor antagonist, used over a range of concentrations (0.1–10 μM), to rescue the motor deficits in an AD model [57]. The worms were placed on NGM plates coated with OP50 *E. coli* bacteria that had been pre-treated with 0.1 M tetramethylrhodamine ethyl ester perchlorate (TMRE) for relative quantitation of mitochondrial membrane potential, the same number protocol was repeated with 10 μM MitoTracker Green FM (Invitrogen, Carlsbad, CA) for assessing mitochondrial density according to methods previously done [58]. The worms were then transferred to fresh NGM plates containing only OP50 *E. coli* for 1 h to clear their intestinal tracts of any remaining dye. Following this, they were

immobilized in situ on the NGM plates by the addition of 10 mg/ml levamisole (Sigma, St. Louis, MO) [58, 59]. It is important to note that the localization of MitoTracker Green FM dye within mitochondria is largely independent of membrane potential, while TMRE dye specifically measures mitochondrial membrane potential. The fluorescence intensity of the terminal pharyngeal bulb (PB) was measured using EVOS FL digital inverted microscope with GFP filter at 4× magnification.

Assessment of nuclei expression using DAPI staining (acetone fixation)

DAPI staining is used to visualize and quantify the number of cells and to assess nuclear integrity [60]. DAPI (4',6-diamidino-2-phenylindole) is a fluorescent stain that binds strongly to DNA, allowing for the identification of nuclei in cell populations. This technique was performed following a previously outlined procedure [61] in the different treatment groups. This method would evaluate and detect nuclear changes in the treated groups and determine the effect of vanadium and therapeutic potentials of ZA-II-05 on cellular health. It would assess nuclear morphology and detect abnormalities in the nucleus, such as fragmentation or condensation, which are indicative of cell stress or damage. To determine the nuclear localization in the different experimental groups at a temperature of 20 °C for 24 h, the acetone fixation method with DAPI staining was employed, as it effectively highlights distinct nuclei in nematodes within a reasonable timeframe (less than 1 h). After treating the worms belonging to different experimental groups, placed on NGM plates coated with OP50 *E. coli* bacteria, they were rinsed off from the plate using M9 buffer. The resulting suspension was then subjected to centrifugation at 1000×g for 60 s, and the supernatant was disposed of. The pellets obtained were washed with 1 mL of dH₂O, collected, and the supernatant was discarded. Subsequently, 400 µL of 30% acetone was added to the pellets and incubated for 15 min. The suspension was then centrifuged at 1000×g for 1 min at room temperature, and the supernatant was discarded. The worms underwent two additional washes with 500 µL of dH₂O, and the supernatant was discarded after each wash. To label the worms, 50 µL of a 4',6-diamidino-2-phenylindole (DAPI) solution (10 µg/mL) was added to the tube and incubated for 15 min. The sample was put in the centrifuge and spun at 1000×g for 60 s, and the supernatant was disposed of. The pellets were washed twice with 500 µL of dH₂O. The worms were subsequently transferred onto glass slides, covered with coverslips, and sealed with transparent nail polish gel. The animals were observed using a fluorescence microscope. Viable neurons in the ventral nerve cord (VNC) were identified by assessing

the morphology and size of the nuclei according to methods described [62]. Photos were captured immediately at 4× magnification using Evos fluorescence FL digital inverted microscope with DAPI filter in a dark room.

Assessment of mitochondrial superoxide levels

Vanadium, a heavy metal and environmental toxicant, triggers oxidative stress by impairing mitochondrial function [9]. Evaluating mitochondrial superoxide levels would help to assess the toxic impact of vanadium and its detrimental effects on mitochondrial health [22]. A reduction in superoxide levels following treatment with ZA-II-05 would indicate its potential therapeutic effectiveness. After 24 h of incubation belonging to the different experimental groups, placed on NGM plates coated with OP50 *E. coli* bacteria, the worms were changed to new plates for an hour to remove any residual dye from their digestive tracts. The worms were then immobilised with levamisole at a concentration of 1 mg/mL. Fluorescence studies were conducted in the different experimental groups in low-light conditions at a temperature of 20 degrees. The mean fluorescence intensity of the terminal pharyngeal bulb (PB) was measured in synchronized young nematodes from all experimental groups after 24 h of exposure to 10 µM MitoSox, following the protocol previously outlined [58]. Photos were captured immediately with an exposure time of 1 s at 4× magnification using Evos fluorescence FL digital inverted microscope with CY5 filter in a dark room.

Microscopy

Microscopy (EVOS FL digital inverted microscope) was utilized to validate the precise subcellular localization of fluorescence within the terminal pharyngeal bulbs (PB) of the worms and the entire anatomy of the worms. Individual worms were exposed for 24 h, either individually or in combination with MitoTracker Dye (Green, Red, or Deep Red, Invitrogen, Molecular Probes, Carlsbad, CA), MitoSOX (Mito-HE), or TMRE. Subsequently, following a 1 h intestinal clearing process using unlabeled *E. coli*, the nematodes were immobilized onto glass slides in 20 µl of 10 mg/ml levamisole. Analysis of the captured images was performed using Image J (<http://rsbweb.nih.gov/ij/>).

Chemotaxis assay

The chemotaxis index (CI) was used to evaluate associative memory (linking salt with food) in various experimental groups, following the methods previously outlined [63]. Synchronized, fully developed adult hermaphrodites were collected from a 60 mm NGM dish into a 2 mL tube and washed four times with M9 buffer, after 24 h of incubation belonging to the different

experimental groups and placed on NGM plates coated with OP50 *E. coli* bacteria. Next, 2 μ L (between 50 and 250 worms in each 2 μ L) of adult worms were transferred onto a chemotaxis dish (a 60 mm NGM agar plate without OP50, with a quadrant layout consisting of two control “C” quadrants and two test “T” quadrants arranged opposite each other). The worms were placed at the origin where the two lines intersect. The agar plate was sectioned into four quadrants, with quadrants A and B containing NaCl as the chemoattractant and quadrants C and D lacking NaCl. Each quadrant was also treated with the anesthetic levamisole to paralyze the worms upon contact. Once the worms and chemoattractant drops were absorbed into the agar, the lids were replaced, and the plates were inverted. Chemotaxis was allowed to proceed for 60 min, after which the plates were transferred to a refrigerator at 4 °C to immobilize the worms. Images of the plates were captured using a camera and analyzed with Fiji software to calculate the chemotaxis index (CI). The chemotaxis index (CI) was calculated based on the obtained data. The results for each plate was calculated as CI (chemotaxis index) = $\frac{(A+B)-(C+D)}{Total}$.

Touch withdrawal assay

Touch withdrawal assay was carried out to assess the nematode’s sensory and neuromuscular responses to mechanical stimuli. This assay helps evaluate the function of sensory neurons, motor neurons, and the overall health of the neuromuscular system [24]. By gently touching the worm with a pin used in insect taxidermy, observation on whether the worm withdraws or changes direction in response to the touch was made. The assay assessed the effects of vanadium and ZA-II-05 on neuronal function and behavioral responses. The touch response of the different experimental groups was assessed using previous protocols [64]. After 24 h of incubation belonging to the different experimental groups and placed on NGM plates coated with OP50 *E. coli* bacteria, the worms were placed in a 24-well plate on a shaker, with appropriate volumes of M9 buffer. Four agar plates, each corresponding to a different treatment group, were retrieved from the refrigerator and allowed to reach room temperature for 30 min before the assay. The worms from each treatment group were pipetted onto the designated plates and allowed to dry using the fume hood to expedite the process. The plates were appropriately labelled. Sterilised platinum wire was utilised to individually pick up worms for the assay. It is important to note that the wire was sterilised before transitioning to different groups. To measure the anterior touch response, worms were gently stroked behind the pharynx, and their responses were observed and recorded. The responses were categorized as follows:

- Responsive (quickly reacts and moves away $\rightarrow +1$)
- Partial response (moves away after 3 strokes $\rightarrow 0.5$)
- Non-responsive (does not move away after 3 strokes $\rightarrow 0$)

This procedure was repeated for a minimum of 20 worms from each group. Each worm was subjected to five anterior tests, unless otherwise specified [65]. A group of 20 worms was evaluated in each session, at least three to five times.

Statistics

The statistical analyses were conducted using Graphpad Prism version 9.5.1 (733) for Windows, Graphpad Software Inc. Data, presented as mean \pm standard deviation (SD), were obtained from a minimum of 6 replicates per group of a minimum of 2500 worms each. One-way Analysis of Variance (ANOVA) was utilized for group comparisons. Tukey’s test was employed to compare the means of individual groups. A significance level of $p \leq 0.05$ was considered statistically significant.

Results

In-vitro hippocampal slice culture neuroprotective effect of ZA-II-05

Neuroprotection occurred as a consequence of the added compound, ZA-II-05 after treatment with the excitotoxin, NMDA (10 μ M). Slice cultures (Fig. 3) showed a visibly reduced fluorescent intensity at 100 μ M and 100 mM concentrations when compared to 10 mM, 10 μ M and the slice cultures that were treated with NMDA alone. It established the effective dose range, and the toxic threshold of ZA-II-05. Additionally, *in-vitro* evaluation of ZA-II-05’s safety, efficacy, and potential side effects was achieved in a controlled and measurable manner.

Concentration–response curve of vanadium on mortality of *C. elegans*

This concentration (100 mM) (Fig. 4) was chosen as it induced neurotoxicity in the worms. The results revealed that 100 mM of NaVO₃ exhibited toxicity and induced partial lethality in the worms (50%).

Growth pattern assessment of *C. elegans* following treatment with vanadium and ZA-II-05

In terms of the growth pattern analysis, we examined the effects of vanadium treatment on the worms at a concentration of 100 mM (Fig. 4). We observed delayed growth, a significant alteration in the body length and body wall of the vanadium-treated worms, additionally, reproductive organs were absent, and the intestine appeared shrunken, displaying characteristics reminiscent of the

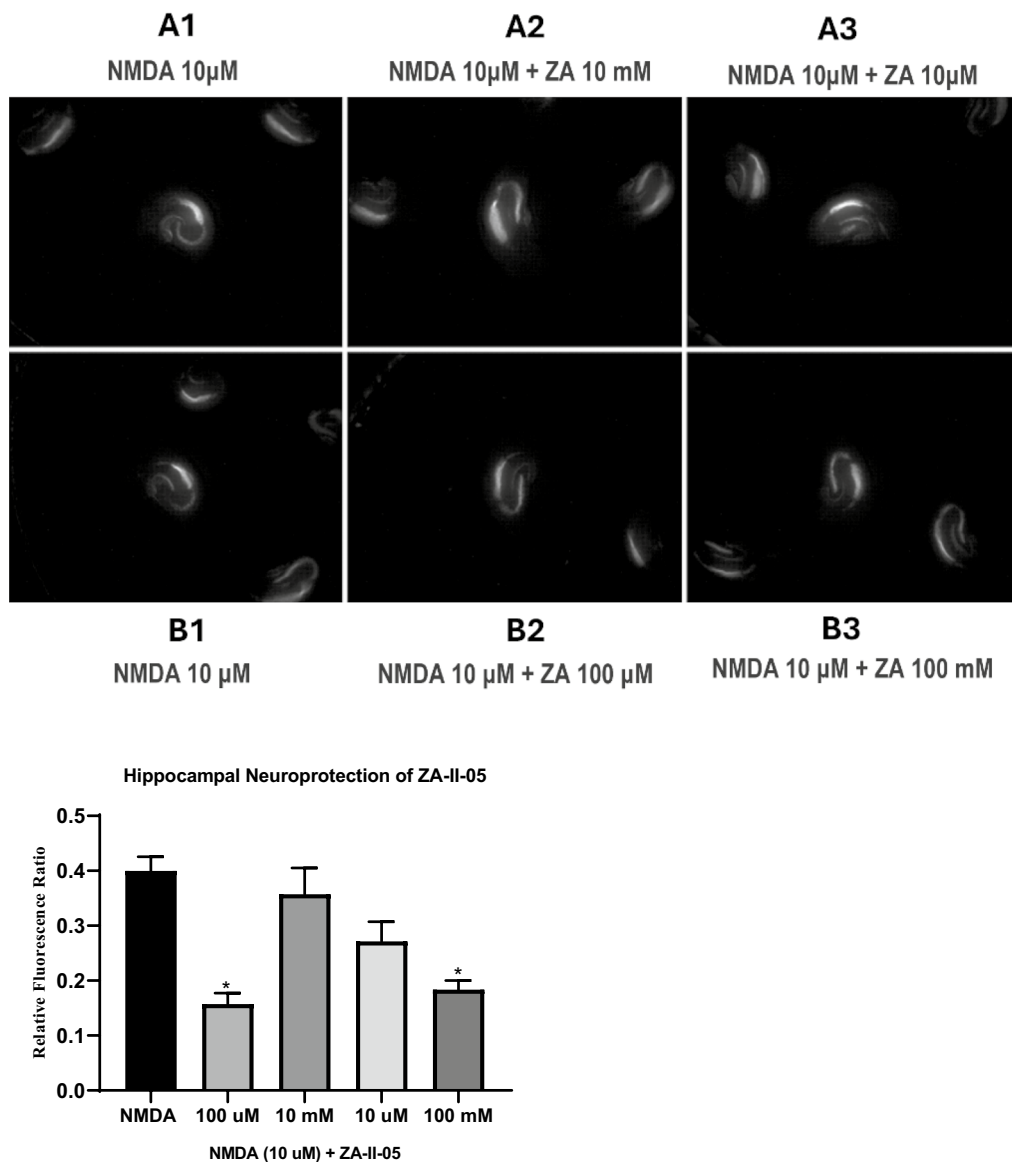


Fig. 3 Neuroprotection against 10 μ M NMDA-insult in organotypic hippocampal slice cultures with different concentrations of ZA-II-05 (10 mM, 10 μ M, 100 Mm). The data analysis revealed that ZA-II-05 exhibited a significant neuroprotective effect at a concentration of 100 μ M and 100 mM, as indicated by a notable decrease in propidium iodide fluorescence intensity compared to the NMDA-treated group. The significance of the observed difference was denoted by the symbol “*”, indicating a statistically significant distinction ($P < 0.05$) compared to the NMDA group. Moreover, the comparison between the 100 mM group and the NMDA group showed a further reduction in propidium iodide fluorescence intensity, signified by the symbol “**”, also indicating a statistically significant difference ($P < 0.05$)

dauer stage of worm development. Co-treatment with ZA-II-05 however reversed this effect (Fig. 5). There was a significant difference in the growth pattern of the control group, compared to the vanadium and ZA-II-05 treated groups. The panels demonstrate the absence of the intestinal tract and reproductive organs in the vanadium-treated group as opposed to the ZA-II-05-treated group. Vanadium treated groups appeared to have

stunted growth patterns with aberrated body wall and body length. Growth patterns were however preserved in ZA-II-05 treated groups.

Relative quantitation of nuclei expression in *C. elegans* by fluorescence microscopy

DAPI staining in the control and ZA-II-05 treated groups consistently showed a highly condensed and

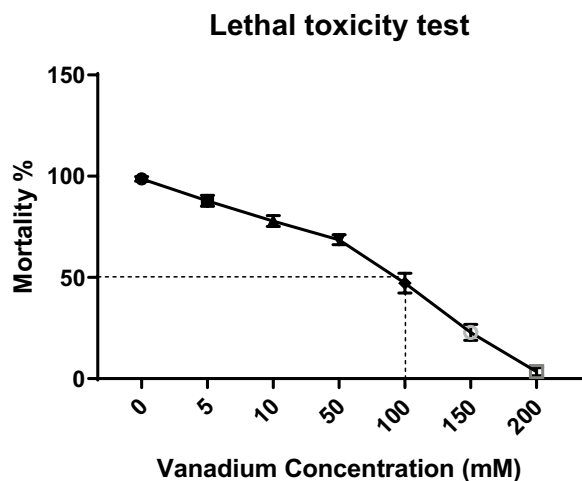


Fig. 4 Depicts the dose response of vanadium in worms. Synchronized L1 worms were subjected to varying concentrations of sodium metavanadate ranging from 0 to 200 mM. A total of 30–60 worms were plated, and the percentage of surviving worms 48 h after treatment was recorded as a measure of lethality. The experiment was repeated six times using independent worms and the mean \pm standard deviation (SD) of $n=6$ was used to determine the lethal toxicity

round fluorescence pattern of nuclei, resembling puncta, compared to vanadium treated worms that showed loss of both hypodermal and neuronal nuclei in the ventral nerve cord. ZA-II-05 treated groups preserved the nucleus. The ventral nerve cord (VNC) encompasses a series of motor neurons that extend along the ventral midline, from the retrovesicular ganglion (RVG) (Insets: Fig. 6A and B). VNC showed a significant loss of both hypodermal (A) and neuronal (B) nucleus in vanadium treated group, there was however a reversal effect in the groups that received ZA-II-05, showing preservation of neuronal morphology, similar to that of control. Approximately more than 50 worms were used in the imaging. Large-scale sample collection is suitable for quantitative analysis (over 50 worms).

Relative quantitation of mitochondrial density in *C. elegans* by fluorescence microscopy

The intensity of fluorescence in the control and ZA-II-05 treated groups indicate a dense presence of mitochondria (Fig. 7). In these groups, the integrity of the intestinal tract and the presence of mitochondria in the pharynx were preserved when compared to the vanadium-treated group. Worms exposed to vanadium showed a decrease or absence of mitochondrial content in the pharyngeal tissue. Both the control group and the group treated with the compound exhibited higher fluorescence density compared to the vanadium treated group. (A) The vanadium-treated group exhibited a significant reduction in

mitochondrial membrane potential (DW_m) compared to the control and ZA-II-05-treated groups. The mean fluorescence in the pharynx and intestinal tract of the vanadium-treated group decreased to 41%. (B) Mitochondrial density in the pharynx was higher in the control and ZA-II-05 treated compared to the vanadium treated groups indicative of cell death. Approximately more than 50 worms were used in the imaging. Large-scale sample collection is suitable for quantitative analysis (over 50 worms).

Relative quantitation of mitochondria superoxide levels *C. elegans* by fluorescence microscopy

To evaluate the levels of oxidants specific to mitochondria, the fluorescent probe MitoSOX Red was utilized. MitoSOX Red is a dye that specifically detects mitochondrial superoxide and emits red fluorescence upon oxidation by superoxide molecules. It can be employed to stain the pharyngeal bulbs of *C. elegans*, which is rich in mitochondria. Notably, both groups of worms treated with vanadium compared to worms treated with ZA-II-05, distinct and prominent fluorescent foci were consistently observed in the densely populated pharyngeal mitochondria region after MitoSOX treatment. Panel (a) shows large fluorescent foci were observed at the pharyngeal mitochondria dense region following MitoSOX treatment for vanadium treated worms as compared to ZA-II-05 treated worms with or without vanadium exposure. Panel (b) shows a light micrograph of an adult wild-type (N2) nematode from vanadium-treated worms, with the cephalad portion (highlighted by a white circle) indicating the two pharyngeal bulbs (m: metacarpus and tb: terminal bulb) and the initial section of the gastrointestinal tract. Approximately more than 50 worms were used in the imaging. Large-scale sample collection is suitable for quantitative analysis (over 50 worms).

Chemotaxis and touch withdrawal behavioral assays

Worms were placed in a defined area, and their response to an odorant (NaCl) was observed. The chemotaxis index (CI) of the ZA-II-05-treated group showed a positive response compared to the group treated with vanadium alone. Interestingly, an impaired response was observed in the chemotaxis index (CI) and touch response of worms exclusively treated with ZA-II-05 when compared to both the control group and the group treated with vanadium + ZA-II-05. Vanadium treated group had lower response to external stimuli as compared to the group treated with ZA-II-05 and control. Not more than 250 worms were used in the chemotaxis assay, crowding can impede worm movement.

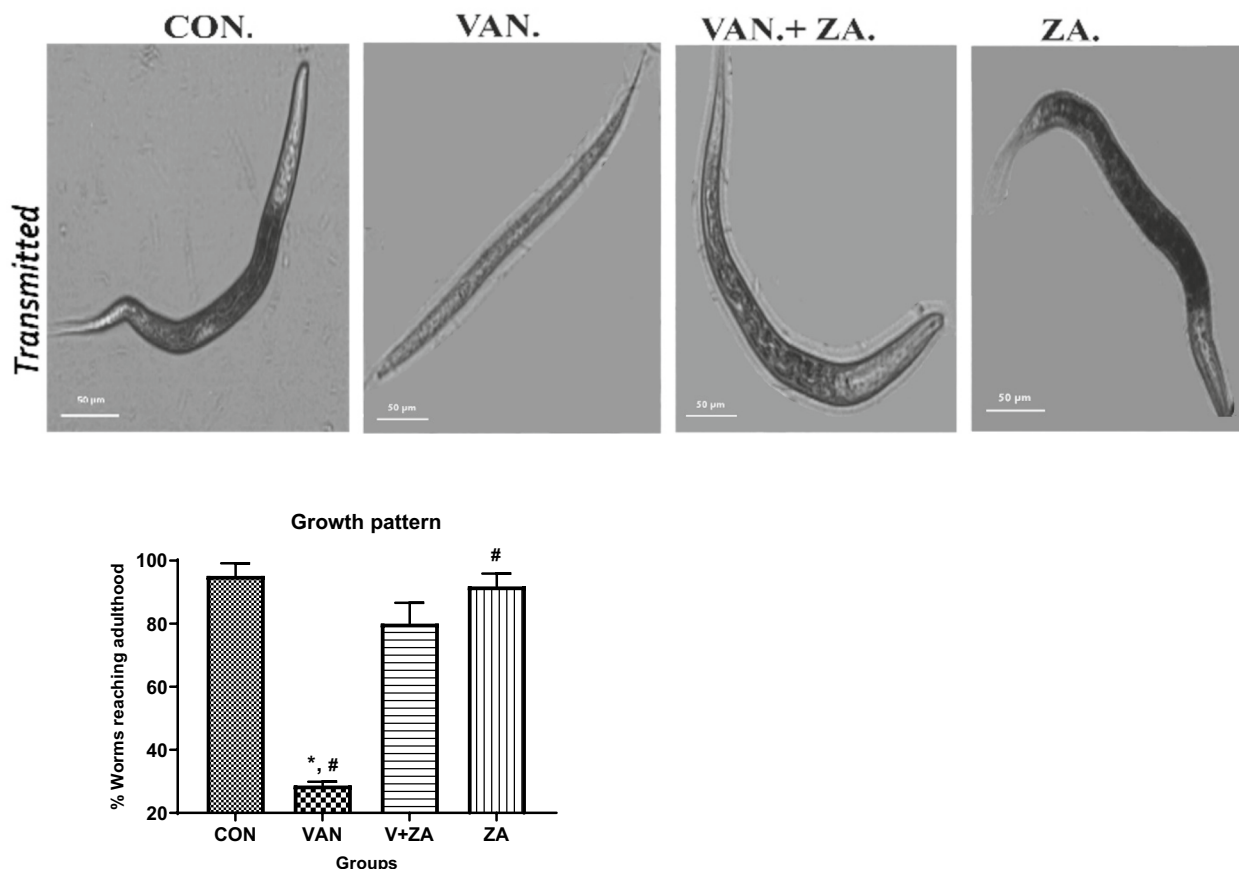


Fig. 5 Illustrates the growth pattern of the worms, revealing a substantial deviation in body length and body wall structure in the vanadium-treated group compared to the ZA-II-05-treated group. The symbol “*” denotes a significant difference compared to the control group at a significance level of $P < 0.05$, while the symbol “#” indicates a significant difference compared to the vanadium + ZA-II-05 (V+ZA) group at the same significance level. Vanadium (100 mM) and ZA-II-05 (1 mg/ml). CON, control; VAN, vanadium; ZA-II-05; ZA. Approximately less than 50 worms were used in the imaging

Discussion

Excessive stimulation of glutamate receptors is recognized as a key factor in neurotoxicity, contributing to the gradual deterioration of neurons. Prior research has demonstrated a progressive loss of apical dendrites and cytotoxic effects in the pyramidal cells of the CA1 and CA3 regions in mice exposed to vanadium [11]. These substantial neuronal losses and alterations in the hippocampus induced by vanadium exposure likely contribute to memory impairment [7]. It has been observed that disturbances in calcium homeostasis

lead to increased production of reactive oxygen species (ROS) through the mitochondrial permeability transition pore, particularly in the CA1 region [66]. The administration of ZA-II-05 displayed neuroprotective properties against neuronal cell death in the pyramidal cells of the prefrontal cortex (PFC) in mice induced by vanadium exposure. This intervention mitigated morphological changes, indicating an enhancement in neuronal functionality. Moreover, it regulated neuroinflammatory responses, thereby shielding neurons from inflammatory damage [11].

(See figure on next page.)

Fig. 6 Fluorescent micrographs of wild-type *Caenorhabditis elegans* (N2) treated vanadium and ZA-II-05, subjected to DAPI staining and subsequently imaged using fluorescent light. Micrographs show parts of the VNC showing neuronal (arrowheads) and hypodermal (arrow) nuclei, note the absence of hypodermal nuclei in the vanadium treated group. The symbol “*” is used to represent a significant difference compared to the control group at a significance level of $P < 0.05$, while the symbol “#” indicates a significant difference compared to vanadium + ZA-II-05 (V+ZA) group at the same significance level. Vanadium (100 mM) and ZA-II-05 (1 mg/ml). CON, control; VAN, vanadium; ZA-II-05; ZA

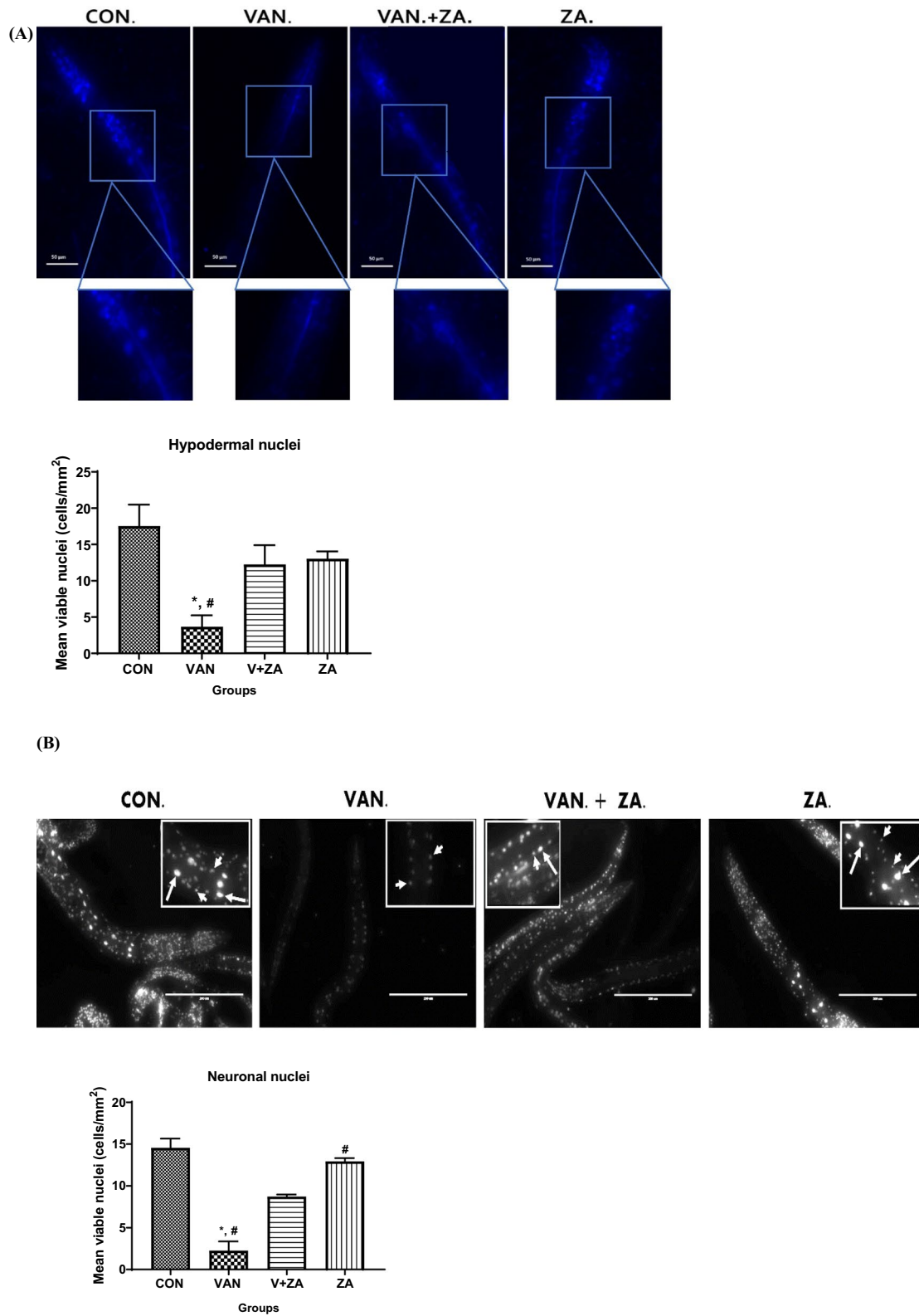


Fig. 6 (See legend on previous page.)

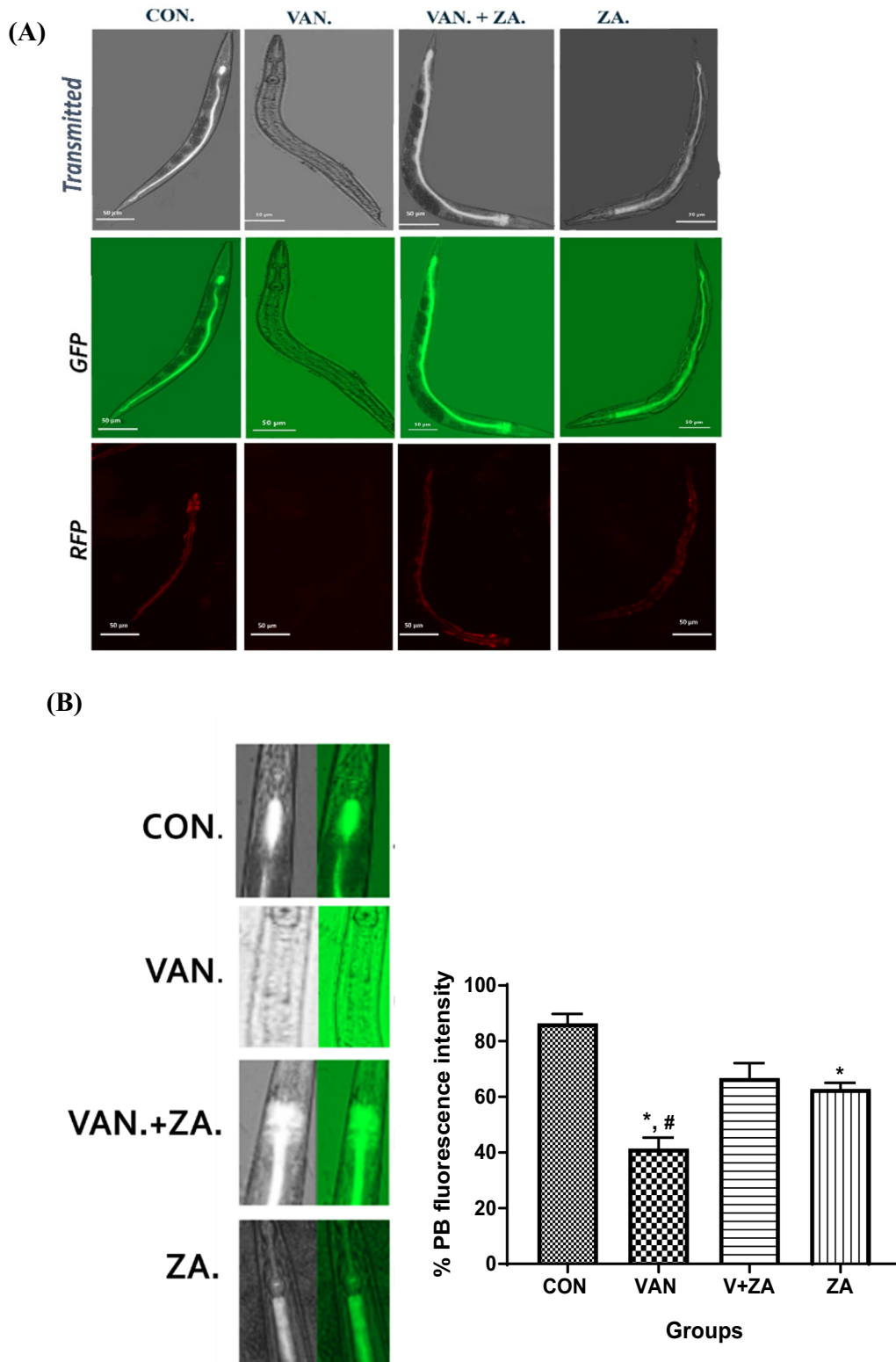


Fig. 7 Illustrates the in vivo quantification of relative mitochondrial potential and mitochondrial density in the terminal pharyngeal bulbs and intestinal tract of *C. elegans* in the different experimental groups. The symbol “**” represents a significant difference compared to the control group at a significance level of $P < 0.05$, while the symbol “#” indicates a significant difference compared to the vanadium + ZA-II-05 (V + ZA) group at the same significance level. The concentrations used were 100 mM for vanadium and 1 mg/ml for ZA-II-05. Abbreviations: CON for control, VAN for vanadium, and ZA for ZA-II-05

In the nematode *C. elegans*, dopamine acts as an essential neurotransmitter, regulating various physiological and behavioral processes within its simple nervous system. It has specific receptors in *C. elegans*, and their functions have been extensively studied [67]. Dopamine, synthesized in dopaminergic neurons like CEP, ADE, and PDE, is involved in locomotion, learning, memory, and response to environmental changes [25, 68]. The DOP-1 dopamine receptor is critical for associative learning, dopamine signaling also contributes to stress responses and thermotaxis [69, 70]. The study of neurotransmitters in *C. elegans* offer valuable insights into their conserved roles in regulating neuronal functions and behavior across organisms and provides a useful model for investigating neurotransmitter signaling and its relevance to human neurological disorders [25, 71]. In the modern era, there has been a utilization of the concept of multi-target-directed ligands (MTDL) [38, 39] to design a variety of compounds that address multiple biological factors linked to neurodegenerative conditions [72–74].

While NMDA receptor antagonists, including ZA-II-05 were primarily developed to interact with NMDA receptors, it also demonstrates a moderate and high affinity also for the dopamine transporter, opioid and sigma receptors, respectively [11]. This phenomenon is commonly referred to as “off-target” binding or cross-reactivity, and it arises due to structural resemblance and shared binding sites [11, 75]. ZA-II-05 underwent evaluation of its binding affinities (K_i) at the PCP site within the NMDAR channel and various neurotransmitter receptors via competitive radioligand binding assays using [^3H]-MK-801 [11]. The studied receptors encompassed 5-HT_{2A}, Dopamine-1 (D₁), Dopamine-2 (D₂), Dopamine Transporter (DAT), Opioid receptors (KOR), μ -opioid receptors (MOR), Norepinephrine Transporter (NET), and Sigma receptor [11]. Notably, ZA-II-05 exhibited notable affinity for Dopamine Transporter (DAT) ($K_i=3161$ nM), Opioid receptors (KOR) ($K_i=361$ nM), μ -opioid receptors (MOR) ($K_i=3038$ nM), and Sigma2 receptor ($K_i=5.5$ nM), demonstrating higher binding affinity compared to other receptors with over 10,000 nM affinity (Ladagu et al., 2023). Moreover, ZA-II-05 display moderate similar affinities for both GluN1/GluN2A and GluN1/GluN2B subtype receptors, with mean IC₅₀ values of 518 nM and 430 nM, respectively [11]. These distinctive attributes likely contributed to more precise and tailored therapeutic interventions against vanadium-induced neurotoxicity in this investigation. A combination of these receptor modulators with NMDA receptor-targeted drugs could potentially yield synergistic effects in certain neuropsychiatric disorders [11].

NIH’s maximal electroshock seizure (MES) assessment of ZA-II-05 revealed its activity at doses of 100 and

300 mg/kg (i.p.) [11]. This substantial protection indicates its anticonvulsant potential, particularly at doses of 100 and 300 mg/kg. ZA-II-05 demonstrated the capability to modulate seizure threshold without impairing locomotion or normal neurological functions. Consistent results across multiple trials validated its efficacy and reliability in targeting seizure activity while preserving regular behavioral and motor functions. ZA-II-05 has been rigorously tested and proven safe for animal experimentation, as endorsed by the NIH approval number: (NIH-6/28/10).

Neuroprotection of ZA-II-05 on hippocampal slices

The use of organotypic hippocampal slice cultures as a model for drug discovery has been extensively reviewed, particularly for studying brain damage, neuroprotection, and neuro-repair [76, 77]. Since the hippocampus is the brain’s memory center, it is commonly used in such in vitro studies. Hippocampal slices retain the natural architecture and cell–cell interactions of brain tissue, making them highly representative of in vivo conditions for assessing drug effects on neurons [78, 79]. The hippocampus, being vulnerable to excitotoxicity, is ideal for testing neuroprotective compounds, providing an ideal model for studying neurodegenerative diseases like Alzheimer’s and Parkinson’s, as well as ischemic brain injury and epilepsy to test the efficacy of drugs targeting these conditions, making it a valuable tool for eliminating harmful compounds early in the drug development process [80, 81].

Drugs that protect neurons from damage, especially against excitotoxicity via NMDA receptor modulation, can be identified through this assay [11, 82]. In this context, the hippocampal slice cultures (Fig. 3) demonstrated that ZA-II-05 provided neuroprotection against NMDA-induced toxicity in rat hippocampal slices. This model has proven to be valuable in investigating NMDA receptor (NMDAR) excitotoxicity and developing neuroprotective strategies [11, 83]. The neuroprotective effect of ZA-II-05 likely stems from its ability to antagonize excitotoxic NMDA receptors, thereby mitigating excitotoxicity—an excessive stimulation of glutamate receptors that can result in neuronal damage and apoptosis [84, 85]. ZA-II-05 demonstrated neuroprotection against NMDA-induced toxicity probably through preservation of calcium ion homeostasis [9].

Growth pattern in *C. elegans* following treatment

Caenorhabditis elegans serves as an effective model for conducting toxicity assessments across its entire life cycle [54]. Growth rate, reproduction, and locomotion are widely used in toxicity evaluation [86]. Recent studies [87] indicate that the p38 and ERK-MAPK signaling

pathways regulate vanadium-induced neurodevelopmental toxicity, potentially impacting growth, mitochondrial function, metal bioavailability, and neurotransmitter levels. The pronounced physical changes in the worms (Fig. 5) could potentially serve as a survival strategy or an adaptive response to cope with the adverse environmental conditions induced by vanadium administration [13, 87]. Furthermore, the vanadium-treated worms exhibited the absence of an intestinal tract and reproductive organs, indicating a disruption in normal growth progression. In contrast, the ZA-II-05 treated group maintained these features, suggesting that ZA-II-05 possesses the ability to mitigate inflammation and oxidative stress, which could otherwise hinder proper growth and development as shown in the measurement of superoxide levels in the worms. Additionally, ZA-II-05 enhanced dopamine signaling which serves as a possible mechanism to ensure that the worms steadfastly remained close to a food source.

Nuclei expression in *C. elegans* following treatment

The organization and distribution of neuronal nuclei within the VNC play a critical role in maintaining neuronal connectivity and function. Both neurons and nuclei in the ventral nerve cord of *C. elegans* provide valuable insights into the molecular and cellular mechanisms underlying neuronal development, function, and plasticity [88]. Putative neurons in the VNC are identified based on the size and morphology of the nuclei [89, 90]. Physical assessment of the worms previously described [81, 91] suggests that the changes observed probably lead to disruptions in their structure and function. Loss of nuclei in the vanadium treated worms possibly lead to defects in axon maintenance within the ventral nerve cord (VNC). Inappropriate or failed gene expression in animals affect the development of the VNC [92, 93]. This can be attributed to the loss of developmental proteins, ultimately resulting in significant disruption of axonal organization in the VNC in the vanadium treated worms [94]. Heavy metal toxicity can have profound effects on the ventral nerve cord of *C. elegans*, causing neuronal degeneration, impaired synaptic transmission, altered morphology, disrupted neuronal activity, and functional impairments in locomotion and behavior which ultimately leads to abnormal movement patterns, paralysis, or altered behavioral responses as observed in our behavioural assays [95]. The preservation of the nucleus in ZA-II-05-treated worms (Fig. 6) is likely attributed to its ability to minimize oxidative damage to the nucleus by preserving redox balance and contributing to the maintenance of nuclear integrity. ZA-II-05 may have also promoted the activity of DNA repair enzymes and facilitated the restoration of damaged DNA [96], which preserves

the structure and function of the nucleus. Additionally, NMDA receptor antagonists have been shown to suppress neuroinflammatory processes, including the release of pro-inflammatory cytokines [97]. By reducing neuroinflammation, these antagonists indirectly protect the nucleus from inflammatory-mediated damage.

Mitochondrial density and membrane potential in *C. elegans* following treatment

C. elegans, exhibit a high concentration of mitochondria in the pharyngeal region the inner membrane potential of mitochondria plays a critical role in determining their function [98, 99]. ZA-II-05 probably preserved mitochondrial density (Fig. 7) by reducing the production of reactive oxygen species (ROS) and enhancing antioxidant defense systems generated by vanadium administration as previously reported [11]. This preservation of redox balance helps protect mitochondrial integrity and maintain mitochondrial density [100, 101]. Additionally, we suggest ZA-II-05 regulated energy metabolism, by promoting mitochondrial respiration and ATP production, this supports and maintains a healthy population of functional mitochondria and preserves mitochondrial density. NMDA receptor antagonists are known to promote mitochondrial quality control mechanisms such as mitophagy, a process by which damaged or dysfunctional mitochondria are selectively removed.

Mitochondria superoxide levels in *C. elegans* following treatment

Numerous studies have indicated a strong association between vanadium toxicity and reactive oxygen species (ROS) [87, 102]. Vanadium exposure has been found to induce cellular apoptosis through increased levels of ROS and ROS-related signaling pathways, but the precise mechanism is not fully understood and requires further investigation [103, 104]. On the other hand, the administration of antioxidants, either as complex ligands [105] or co-administered compounds [106], has shown significant reduction in vanadium toxicity [107, 108]. The high intensity of fluorescence (Fig. 8) indicates an elevated production of reactive oxygen species (ROS) and consequently oxidative stress, potentially attributing it to vanadium's ability to cause cellular hypoxia. This effect was however alleviated by ZA-II-05. Therefore, we can infer that ZA-II-05 likely possesses antioxidative and anti-inflammatory properties. NMDA receptor antagonists have been found to preserve mitochondrial function by preventing calcium overload [11], which can disrupt mitochondrial integrity and enhance ROS production [109]. By maintaining mitochondrial function, NMDA receptor antagonists contribute to the reduction of oxidative stress. Overall, we propose that ZA-II-05 exhibited

anti-oxidative properties by attenuating excitotoxicity, modulating calcium homeostasis, inhibiting NOS activity, suppressing inflammation, and protecting mitochondrial function.

Chemotaxis and touch withdrawal response

Caenorhabditis elegans, with its well-characterized nervous system, transparency, short life cycle, and genetic manipulability, serves as an excellent model organism for studying the molecular and circuitry aspects of mechanosensation [21]. Numerous studies in literature have utilized behavioral changes in *C. elegans* as an indicator for neurotoxicity assessment. Previous findings showed behavioral deficit (reduced movement) observed after just 4 h of exposure to heavy metals, lead (Pb) and copper (Cu) [110].

This positive chemotaxis index (Fig. 9) may be attributed to the preservation of the ventral nerve cord, as indicated by DAPI staining. ZA-II-05 might have mitigated this damage by modulating and preserving the normal function of chemosensory neurons and downstream signaling pathways involved in chemotaxis. Additionally, previous studies have shown that NMDARs are a requirement for the memory component of salt chemotaxis learning (Kano et al., 2008). The DOP-1 dopamine receptor has also been shown to be critical for associative learning. Dopamine signaling also contributes to stress responses and thermotaxis [111]. The impaired movement observed in the touch withdrawal assay aligns with the findings from the DAPI stain, which revealed damage to the ventral nerve cord (VNC) responsible for overall movement control. Disrupted wiring in the motor circuitry likely contributed to the impaired movement [112]. Neurotoxicity due to vanadium led to impaired sensory neurons, which probably resulted in reduced touch sensitivity and delayed or absent response [113], while motor neuron damage probably reduced the worms' ability to move properly [114]. The touch withdrawal behavior detected and quantified the effects of vanadium, leading to dysfunction in the nervous system that reflected in altered or absent responses to touch stimuli [25]. In contrast, treatment with ZA-II-05 significantly restored touch sensitivity. The specific mechanisms by which ZA-II-05 exerted its protective effects on chemotaxis

and touch response are not fully understood and may involve multiple cellular and molecular pathways. Further research is necessary to unravel the precise mechanisms underlying the preservation of chemotaxis and touch response by ZA-II-05 in vanadium-treated worms.

Notably, previous investigations conducted in our laboratory have indicated that the administration of antioxidants can exhibit prooxidative effects in the absence of stressors, such as vanadium, as previously reported [115]. The absence of neurotoxic effects from vanadium, such as the generation of reactive oxygen species (ROS) for the compound to counteract, resulted in neurotoxicity as observed in the group that was treated with ZA-II-05 only especially in the chemotaxis assay (Fig. 9). Additionally, this outcome could be attributed to the concentration of ZA-II-05 exceeding a neuroprotective threshold in the absence of a neurotoxicant. It's worth noting that a prior study demonstrated that a high concentration of dietary glucose (250 mM) fails to confer protection against polyglutamine toxicity [116]. This discrepancy may arise from the utilization of polyglutamine constructs with varying lengths or the possibility that the concentration of glucose does not exhibit neuroprotective effects beyond a certain threshold concentration.

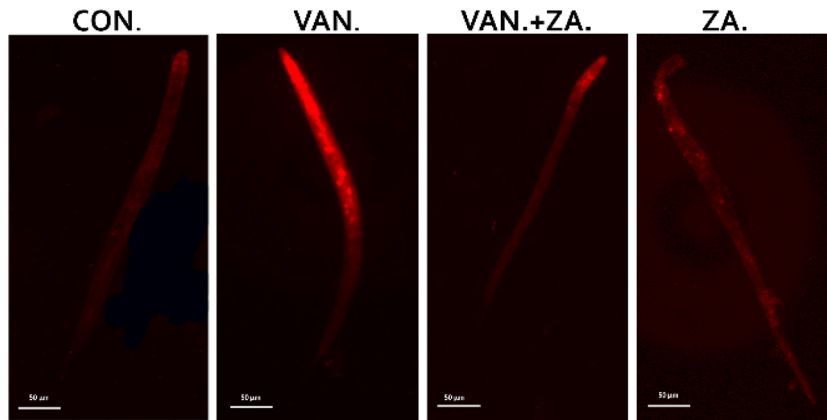
Conclusions

In conclusion, our investigation into the neurotoxic effects of vanadium and the potential neuroprotective role of the mixed glutamate-dopamine drug, ZA-II-05, in the model organism *Caenorhabditis elegans* has yielded valuable insights into the consequences of vanadium exposure and the prospects for mitigating its harmful impact. The results of our study were compelling, not only shedding light on the mechanisms underlying vanadium-induced neurotoxicity but also offering promising perspectives for the development of therapeutic interventions. By exploring the potential of NMDA receptor and dopamine modulation in countering the toxic effects of vanadium exposure, we contribute to the broader understanding of neurotoxicity, particularly in the context of environmental toxins. Ultimately, our study underscores the importance of continued research into innovative strategies for addressing the complex interplay between environmental toxins and neurological well-being.

(See figure on next page.)

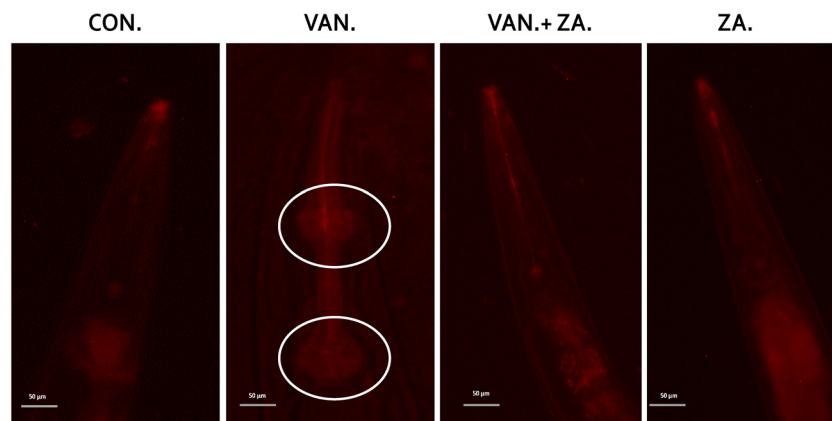
Fig. 8 Illustrates the labeling of nematode terminal pharyngeal bulbs using mitochondria-targeted dyes (MitoSOX) to measure superoxide levels. MitoSOX fluorescence demonstrates consistent labeling within the *C. elegans* pharynx, with a particular emphasis on the terminal pharyngeal bulb. A magnified image at 40× magnification is presented, captured using a CY5 filter. The symbol "*" is used to represent a significant difference compared to the control group at a significance level of $P < 0.05$, while the symbol "#" indicates a significant difference compared to vanadium + ZA-II-05 (V + ZA) group at the same significance level. Vanadium (100 mM) and ZA-II-05 (1 mg/ml). CON, control; VAN, vanadium; ZA-II-05; ZA

(A)



C. elegans superoxide levels after treatment with Vanadium and ZA-II-05

(B)



C. elegans superoxide levels after treatment with Vanadium and ZA-II-05.

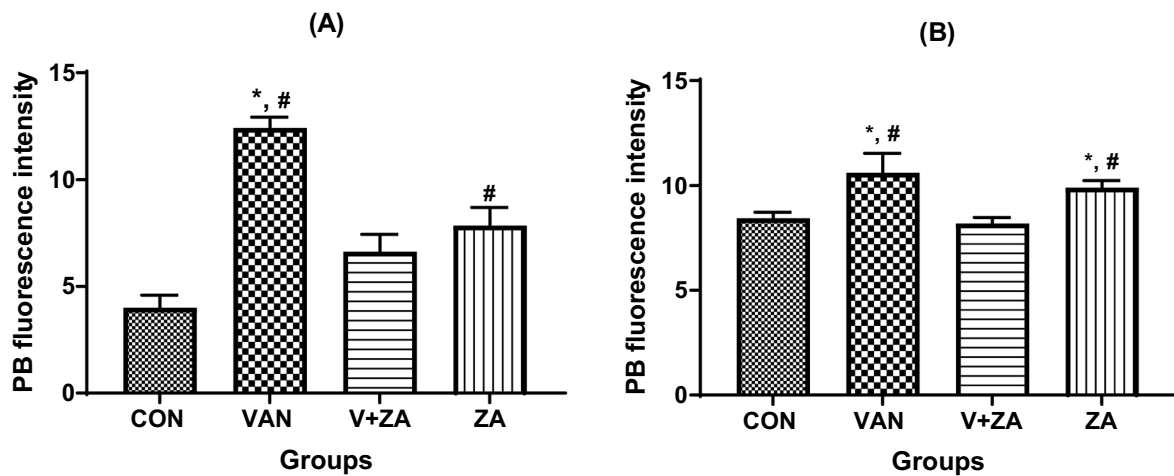


Fig. 8 (See legend on previous page.)

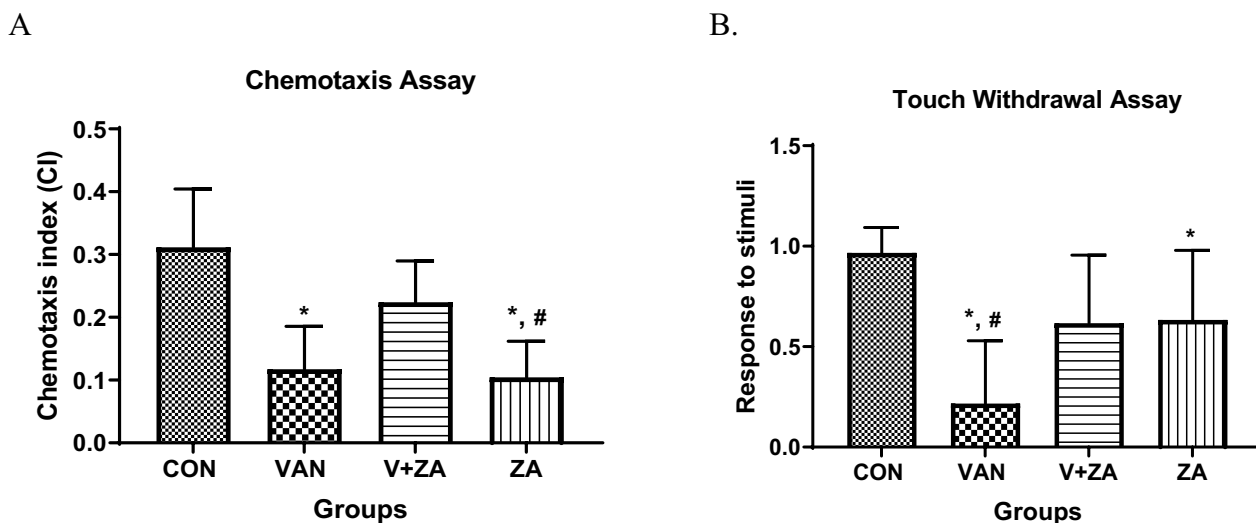


Fig. 9 Illustrates **A** Chemotaxis Assay: Measurement of memory associated with food; Vanadium treated group had significantly lower chemotaxis index (CI) compared to the control and ZA-II-05 treated groups. **B** Touch Withdrawal: The symbol "*" is used to represent a significant difference compared to the control group at a significance level of $P < 0.05$, while the symbol "#" indicates a significant difference compared to vanadium + ZA-II-05 (V + ZA) group at the same significance level. Vanadium (100 mM) and ZA-II-05 (1 mg/ml). CON, control; VAN, vanadium; ZA; ZA-II-05

Acknowledgements

The authors would like to appreciate Saint Joseph's University for their support to this project

Author contributions

AD conducted the research and wrote the manuscript, TG, FO and PC edited the manuscript, TE, TL, MF, EH, JM and ZA conducted some experiments, AA and JO designed the work.

Funding

There was no external funding. Open Access funding enabled and organized by Adeboye Adejare.

Data availability

No datasets were generated or analysed during the current study.

Declarations

Ethics approval and consent to participate

Approval for the study was obtained from the University of Ibadan Animal Care and Use Research Ethics Committee (UI-ACUREC) with the reference number UI- ACUREC/17/0035.

Consent for publication

Not applicable.

Competing interests

The authors declare no competing interests.

Author details

¹Department of Veterinary Anatomy, University of Ibadan, Ibadan, Nigeria. ²Department of Anatomy, College of Medicine, University of Ibadan, Ibadan, Nigeria. ³Department of Biosciences, Durham University, County Durham DH1 3LE, UK. ⁴Department of Pharmacognosy, Faculty of Pharmacy, University of Ibadan, Ibadan, Oyo, Nigeria. ⁵Department of Neuroscience, College of Arts and Sciences, Saint Joseph's University, Philadelphia, PA, USA. ⁶Department of Pharmaceutical Sciences, Philadelphia College of Pharmacy, Saint Joseph's University, Philadelphia, PA, USA. ⁷Department of Pharmaceutical Chemistry, Ankara University, Ankara, Turkey.

Received: 31 May 2024 Accepted: 25 September 2024

Published online: 28 October 2024

References

- Usende IL, Olopade JO, Emikpe BO, Oyagbemi AA, Adedapo AA. Oxidative stress changes observed in selected organs of African giant rats (*Cricetomys gambianus*) exposed to sodium metavanadate. *Int J Vet Sci Med.* 2018;6(1):80–9.
- Afeseh Ngwa H, Kanthasamy A, Anantharam V, Song C, Witte T, Houk R, Kanthasamy AG. Vanadium induces dopaminergic neurotoxicity via protein kinase Cdelta dependent oxidative signaling mechanisms: relevance to etiopathogenesis of Parkinson's disease. *Toxicol Appl Pharmacol.* 2009;240(2):273–85. <https://doi.org/10.1016/j.taap.2009.07.025>.
- Olopade JO, Mustapha OA, Fatola OI, Ighorodje E, Folarin OR, Olopade FE, Omile IC, Obasa AA, Oyagbemi AA, Olude MA, Thackray AM. Neuropathological profile of the African giant rat brain (*Cricetomys gambianus*) after natural exposure to heavy metal environmental pollution in the Nigerian Niger delta. *Environ Sci Poll Res.* 2023. <https://doi.org/10.1007/s11356-023-30619-0>.
- Mustapha OA, Olude MA, Bello ST, Taiwo A, Jagun A, Olopade JO. Peripheral axonopathy in sciatic nerve of adult Wistar rats following exposure to vanadium. *J Peripher Nerv Syst.* 2019;24(1):94–9.
- Ohiomokhare S, Olaolorun F, Ladagu A, Olopade F, Howes MJR, Okello E, Olopade J, Chazot PL. The pathopharmacological interplay between vanadium and iron in Parkinson's disease models. *Int J Mol Sci.* 2020;21(18):6719.
- Olaolorun FA, Olopade FE, Usende IL, Lijoka AD, Ladagu AD, Olopade JO. Neurotoxicity of vanadium. In: Olaolorun FA, Olopade FE, Usende IL, Lijoka AD, Ladagu AD, Olopade JO, editors. *Advances in neurotoxicology*, vol. 5. Cambridge: Academic Press; 2021. p. 299–327.
- Folarin OR, Snyder AM, Peters DG, Olopade F, Connor JR, Olopade JO. Brain metal distribution and neuro-inflammatory profiles after chronic vanadium administration and withdrawal in mice. *Front Neuroanat.* 2017;11:58.

8. Xiong Z, Xing C, Xu T, Yang Y, Liu G, Hu G, Cao H, Zhang C, Guo X, Yang F. Vanadium induces oxidative stress and mitochondrial quality control disorder in the heart of ducks. *Front Vet Sci.* 2021;8: 756534.
9. Ladagu AD, Olopade FE, Folarin OR, Elufioye TO, Wallach JV, Dybek MB, Olopade JO, Adejare A. Novel NMDA-receptor antagonists ameliorate vanadium neurotoxicity. *Naunyn Schmiedebergs Arch Pharmacol.* 2020;393:1729–38.
10. Hao Y, Xiong R, Gong X. Memantine, NMDA receptor antagonist, attenuates ox-LDL-induced inflammation and oxidative stress via activation of BDNF/TrkB signaling pathway in HUVECs. *Inflammation.* 2021. <https://doi.org/10.1007/s10753-020-01365-z>.
11. Ladagu AD, Olopade FE, Chazot P, Oyagbemi AA, Ohiomokhare S, Folarin OR, Gilbert TT, Fuller M, Luong T, Adejare A, Olopade JO. Attenuation of vanadium-induced neurotoxicity in rat hippocampal slices (in vitro) and mice (in vivo) by ZA-II-05, a novel NMDA-receptor antagonist. *Int J Mol Sci.* 2023;24:16710. <https://doi.org/10.3390/ijms242316710>.
12. Shukla AK, Wodrich AP, Sharma A, Giniger E. Invertebrate models in translational research: lessons from *Caenorhabditis elegans* and *Drosophila melanogaster*. In: Shukla AK, Wodrich AP, Sharma A, Giniger E, editors. *Biotechnology in healthcare.* Cambridge: Academic Press; 2022. p. 31–48.
13. Ijomone OM, Miah MR, Peres TV, Nwoha PU, Aschner M. Null allele mutants of trt-1, the catalytic subunit of telomerase in *Caenorhabditis elegans*, are less sensitive to Mn-induced toxicity and DAergic degeneration. *Neurotoxicology.* 2016;57:54–60.
14. Zhen M, Samuel AD. *Caenorhabditis elegans* locomotion: small circuits, complex functions. *Curr Opin Neurobiol.* 2015;33:117–26.
15. Bono MD, Villu Maricq A. Neuronal substrates of complex behaviors in *C. elegans*. *Annu Rev Neurosci.* 2005;28(1):451–501.
16. Hobert O. The neuronal genome of *Caenorhabditis elegans*. *WormB Online Rev C Elegans Biol.* 2018. <https://doi.org/10.1895/wormbook.1.161.1>.
17. Tsalik EL, Hobert O. Functional mapping of neurons that control locomotory behavior in *Caenorhabditis elegans*. *J Neurobiol.* 2003;56(2):178–97.
18. DiLoreto EM, Chute CD, Bryce S, Srinivasan J. Novel technological advances in functional connectomics in *C. elegans*. *J Dev Biol.* 2019;7(2):8.
19. Hobert O. A map of terminal regulators of neuronal identity in *Caenorhabditis elegans*. *Wiley Interdiscip Rev Dev Biol.* 2016;5(4):474–98.
20. Hobert O, Glenwinkel L, White J. Revisiting neuronal cell type classification in *Caenorhabditis elegans*. *Curr Biol.* 2016;26(22):R1197–203.
21. Sastre J, Pallardó FV, Viña J. *Free Radical Biol. Med.* 2003;35:1–8.
22. Caito SW, Aschner M. NAD⁺ supplementation attenuates methylmercury dopaminergic and mitochondrial toxicity in *Caenorhabditis Elegans*. *Toxicol Sci.* 2016;151(1):139–49. <https://doi.org/10.1093/toxsci/kfw030>.
23. Kano T, Brockie PJ, Sassa T, Fujimoto H, Kawahara Y, Iino Y, Mellem JE, Madsen DM, Hosono R, Maricq AV. Memory in *Caenorhabditis elegans* is mediated by NMDA-type ionotropic glutamate receptors. *Curr Biol.* 2008;18(13):1010–5. <https://doi.org/10.1016/j.cub.2008.05.051>.
24. Campbell JC, Chin-Sang ID, Bendena WG. Mechanosensation circuitry in *Caenorhabditis elegans*: a focus on gentle touch. *Peptides.* 2015;68:164–74.
25. Sanyal S, Wintle RF, Kindt KS, Nuttley WM, Arvan R, Fitzmaurice P, Bigras E, Merz DC, Hébert TE, van der Kooy D, Schafer WR. Dopamine modulates the plasticity of mechanosensory responses in *Caenorhabditis elegans*. *EMBO J.* 2004;23(2):473–82.
26. Felton CM, Johnson CM. Dopamine signaling in *C. elegans* is mediated in part by HLH-17-dependent regulation of extracellular dopamine levels. *G3 Genes Genomes Genetics.* 2014;4(6):1081–9.
27. Choi YK, Tarazi FI. Alterations in dopamine and glutamate neurotransmission in tetrahydrobiopterin deficient spr2/2 mice: relevance to schizophrenia. *BMB Rep.* 2010;43:593–8.
28. Xie W, Li X, Li C, Zhu W, Jankovic J, et al. Proteasome inhibition modeling nigral neuron degeneration in Parkinson's disease. *J Neurochem.* 2010;115:188–99.
29. Chase DL, Koelle MR. Biogenic amine neurotransmitters in *C. elegans*. *WormB Feb.* 2007;20:1–15.
30. Tang B, Tong P, Xue KS, Williams PL, Wang JS, Tang L. High-throughput assessment of toxic effects of metal mixtures of cadmium (Cd), lead (Pb), and manganese (Mn) in nematode *Caenorhabditis elegans*. *Chemosphere.* 2019;234:232–41.
31. Melnikov K, KucharikováBárdyováBotekKaiglová SZNA. Applications of a powerful model organism *Caenorhabditis elegans* to study the neurotoxicity induced by heavy metals and pesticides. *Physiol Res.* 2023;72(2):149.
32. Avila D, Helmcke K, Aschner M. The *Caenorhabditis elegans* model as a reliable tool in neurotoxicology. *Hum Exp Toxicol.* 2012;31(3):236–43.
33. Soares FA, Fagundes DA, Avila DS. Neurodegeneration induced by metals in *Caenorhabditis elegans*. In: Soares FA, Fagundes DA, Avila DS, editors. *Neurotoxicity of metals.* Cham: Springer International Publishing; 2017. p. 355–83.
34. Helmcke KJ, Avila DS, Aschner M. Utility of *Caenorhabditis elegans* in high throughput neurotoxicological research. *Neurotoxicol Teratol.* 2010;32(1):62–7.
35. Ruzsiewicz JA, Pinkas A, Miah MR, Weitz RL, Lawes MJ, Akinyemi AJ, Ijomone OM, Aschner M. *C. elegans* as a model in developmental neurotoxicology. *Toxicol Appl Pharmacol.* 2018;354:126–35.
36. Leung MC, Williams PL, Benedetto A, Au C, Helmcke KJ, Aschner M, Meyer JN. *Caenorhabditis elegans*: an emerging model in biomedical and environmental toxicology. *Toxicol Sci.* 2008;106(1):5–28.
37. Du M, Wang D. The neurotoxic effects of heavy metal exposure on GABAergic nervous system in nematode *Caenorhabditis elegans*. *Environ Toxicol Pharmacol.* 2009;27(3):314–20.
38. González JF, Alcántara AR, Doadrio AL, Sánchez-Montero JM. Developments with multi-target drugs for Alzheimer's disease: an overview of the current discovery approaches. *Expert Opin Drug Discov.* 2019;14(9):879–91.
39. Makhoba XH, Viegas C Jr, Mosa RA, Viegas FP, Poole OJ. Potential impact of the multi-target drug approach in the treatment of some complex diseases. *Drug Des Dev Therapy.* 2020. <https://doi.org/10.2147/DDDT.S257494>.
40. Rodríguez-Soacha DA, Scheiner M, Decker M. Multi-target-directed-ligands acting as enzyme inhibitors and receptor ligands. *Eur J Med Chem.* 2019;180:690–706.
41. Alaeddine RA, Elzahhar PA, AlZaim I, Abou-Kheir W, Belal AS, El-Yazbi AF. The emerging role of COX-2, 15-LOX and PPAR γ in metabolic diseases and cancer: an introduction to novel multi-target directed ligands (MTDLs). *Curr Med Chem.* 2021;28(11):2260–300.
42. Bolognesi ML, Rosini M, Andrisano V, Bartolini M, Minarini A, Tumiatti V, Melchiorre C. MTDL design strategy in the context of Alzheimer's disease: from lipocrine to memoquin and beyond. *Curr Pharm Des.* 2009;15(6):601–13.
43. Dias KST, Viegas C. Multi-target directed drugs: a modern approach for design of new drugs for the treatment of Alzheimer's disease. *Curr Neuropharmacol.* 2014;12(3):239–55.
44. Zhou J, Jiang X, He S, Jiang H, Feng F, Liu W, Qu W, Sun H. Rational design of multitarget-directed ligands: strategies and emerging paradigms. *J Med Chem.* 2019;62(20):8881–914.
45. Boyenoh G, Zeynep A, Adeboye A. Bicyclo-heptan-2-amines; USA Patent # 8,735,590 B2. 2014.
46. Norberg J, Kristensen BW, Zimmer J. Markers for neuronal degeneration in organotypic slice cultures. *Brain Res Protoc.* 1999;3:278–90.
47. Norberg J, Poulsen FR, Blaabjerg M, Kristensen BW, Bonde C, Montero M, Meyer M, Gramsbergen JB, Zimmer J. Organotypic hippocampal slice cultures for studies of brain damage, neuroprotection and neurorepair. *Curr Drug Target CNS Neurol Disord.* 2005;4(4):435–52.
48. Saunders-Mattingly MA. Discovery of natural product analogs against ethanol-induced cytotoxicity in hippocampal slice cultures. 2018.
49. Ramírez-Sánchez J, Pires ENS, Nuñez-Figueroa Y, Pardo-Andreu GL, Fonseca-Fonseca LA, Ruiz-Reyes A, Ochoa-Rodríguez E, Verdecia-Reyes Y, Delgado-Hernández R, Souza DO, Salbego C. Neuroprotection by JM-20 against oxygen-glucose deprivation in rat hippocampal slices: Involvement of the Akt/GSK-3 β pathway. *Neurochem Int.* 2015;90:215–23.
50. Stiernagle T. Maintenance of *C. elegans*. *WormBook.* 2006. <https://doi.org/10.1895/wormbook.1.101.1>.
51. Ijomone OM, Miah MR, Akingbade GT, Bucinca H, Aschner M. Nickel-induced developmental neurotoxicity in *C. elegans* includes cholinergic, dopaminergic and GABAergic degeneration, altered behaviour, and increased SKN-1 activity. *Neurotox Res.* 2020;37:1018–28.

52. Anderson GL, Boyd WA, Williams PL. Assessment of sublethal endpoints for toxicity testing with the nematode *Caenorhabditis elegans*. *Environ-Toxicol Chem Int J*. 2001;20(4):833–8.
53. Augsten LV, Das Neves GM, Gonçalves IL, De Souza JP, Garcia SC, Eiffer-Lima VL. The role of alternative toxicological trials in drug discovery programs. The case of *Caenorhabditis elegans* and other methods. *Curr Med Chem*. 2022;29(32):5270–88.
54. Li WH, Ju YR, Liao CM, Liao VHC. Assessment of selenium toxicity on the life cycle of *Caenorhabditis elegans*. *Ecotoxicology*. 2014;23:1245–53.
55. Corsi AK. A biochemist's guide to *C. elegans*. *Anal biochem*. 2006;359(1):1.
56. Martins AC, Virgolini MB, Ávila DS, Scharf P, Li J, Tinkov AA, Skalny AV, Bowman AB, Rocha JB, Aschner M. Mitochondria in the spotlight: *C. elegans* as a model organism to evaluate xenobiotic-induced dysfunction. *Cells*. 2023;12(17):2124.
57. Turcu AL, Companys-Alemay J, Phillips MB, Patel DS, Griñán-Ferré C, Loza MI, Brea JM, Pérez B, Soto D, Sureda FX, Kurnikova MG. Design, synthesis, and in vitro and in vivo characterization of new memantine analogs for Alzheimer's disease. *Eur J Med Chem*. 2022;236: 114354.
58. Dingley S, Polyak E, Lightfoot R, Ostrovsky J, Rao M, Greco T, Ischiropoulos H, Falk MJ. Mitochondrial respiratory chain dysfunction variably increases oxidant stress in *Caenorhabditis elegans*. *Mitochondrion*. 2010;10(2):125–36.
59. Scaduto RC, Grotyohann LW. Measurement of mitochondrial membrane potential using fluorescent rhodamine derivatives. *Biophys J*. 1999;76(1):469–77.
60. McGee MD, Weber D, Day N, Vitelli C, Crippen D, Herndon LA, Hall DH, Melov S. Loss of intestinal nuclei and intestinal integrity in aging *C. elegans*. *Aging cell*. 2011;10(4):699–710.
61. Liang J, De Castro A, Flores L. Detecting protein subcellular localization by green fluorescence protein tagging and 4',6'-diamidino-2-phenylindole staining in *Caenorhabditis elegans*. *J Vis Exp*. 2018;137: e57914. <https://doi.org/10.3791/57914>.
62. Han Z, Boas S, Schroeder NE. Corrigendum: unexpected variation in neuroanatomy among diverse nematode species. *Front Neuroanat*. 2016;10:52. <https://doi.org/10.3389/fnana.2016.00052>.
63. Margie O, Palmer C, Chin-Sang I. *Caenorhabditis elegans* chemotaxis assay. *JoVE J Vis Exp*. 2013;74:e50069.
64. Chalfie M, Sulston J. Developmental genetics of the mechanosensory neurons of *Caenorhabditis elegans*. *Dev Biol*. 1981;82:358–70.
65. Hobert O, Tessmar K, Ruvkun G. The *Caenorhabditis elegans* lim-6 LIM homeobox gene regulates neurite outgrowth and function of particular GABAergic neurons. *Development*. 1999;126(7):1547–62.
66. Gustav M, Hans F, Magnus H, Eskil E, Tadeusz W. Flow cytometric analysis of mitochondria from CA1 and CA3 regions of rat hippocampus reveals differences in permeability transition pore activation. *J Neurochem*. 2003;87:532–44.
67. Chalfie M, Sulston JE, White JG, Southgate E, Thomson JN, Brenner S. *J Neurosci*. 1985;5:956–64.
68. Eisenmann DM. Wnt signalling. *WormBook*. 2005. <https://doi.org/10.1895/wormbook.1.7.1>.
69. Raj . Role of dopamine signalling in olfactory learning and in augmenting manganese mediated neurodegeneration in *Caenorhabditis elegans* (Doctoral dissertation, SCTIMST). 2021.
70. Rahmani A, Chew YL. Investigating the molecular mechanisms of learning and memory using *Caenorhabditis elegans*. *J Neurochem*. 2021;159(3):417–51.
71. Ranganathan R, Sawin ER, Trent C, Horvitz HR. Mutations in the *Caenorhabditis elegans* serotonin reuptake transporter MOD-5 reveal serotonin-dependent and-independent activities of fluoxetine. *J Neurosci*. 2001;21(16):5871–84.
72. Ranganathan R, Cannon SC, Horvitz HR. MOD-1 is a serotonin-gated chloride channel that modulates locomotory behaviour in *C. elegans*. *Nature*. 2000;408:470–5.
73. Cavalli A, Bolognesi ML. Neglected tropical diseases: multi-target-directed ligands in the search for novel lead candidates against *Trypanosoma* and *Leishmania*. *J Med Chem*. 2009;52(23):7339–59.
74. Kumar B, Thakur A, Dwivedi AR, Kumar R, Kumar V. Multi-target-directed ligands as an effective strategy for the treatment of Alzheimer's disease. *Curr Med Chem*. 2022;29(10):1757–803.
75. Chartier M, Morency LP, Zylber MI, Najmanovich RJ. Large-scale detection of drug off-targets: hypotheses for drug repurposing and understanding side-effects. *BMC Pharmacol Toxicol*. 2017;18:1–16.
76. Holopainen IE. Organotypic hippocampal slice cultures: a model system to study basic cellular and molecular mechanisms of neuronal cell death, neuroprotection, and synaptic plasticity. *Neurochem Res*. 2005;30:1521–8.
77. Humpel C. Organotypic brain slice cultures: a review. *Neuroscience*. 2015;305:86–98.
78. Kim H, Kim E, Park M, Lee E, Namkoong K. Organotypic hippocampal slice culture from the adult mouse brain: a versatile tool for translational neuropsychopharmacology. *Prog Neuropsychopharmacol Biol Psychiatry*. 2013;41:36–43.
79. Li Q, Han X, Wang J. Organotypic hippocampal slices as models for stroke and traumatic brain injury. *Mol Neurobiol*. 2016;53:4226–37.
80. Su T, Paradiso B, Long YS, Liao WP, Simonato M. Evaluation of cell damage in organotypic hippocampal slice culture from adult mouse: a potential model system to study neuroprotection. *Brain Res*. 2011;1385:68–76.
81. Croft CL, Futch HS, Moore BD, Golde TE. Organotypic brain slice cultures to model neurodegenerative proteinopathies. *Mol Neurodegener*. 2019;14:1–11.
82. Ring A, Tanso R, Noraberg J. The use of organotypic hippocampal slice cultures to evaluate protection by non-competitive NMDA receptor antagonists against excitotoxicity. *Altern Lab Anim*. 2010;38(1):71–82.
83. Lipton SA. Paradigm shift in neuroprotection by NMDA receptor blockade: memantine and beyond. *Nat Rev Drug Discov*. 2006;5(2):160–70.
84. Parsons CG, Danysz W, Quack G. Memantine is a clinically well tolerated N-methyl-D-aspartate (NMDA) receptor antagonist—a review of preclinical data. *Neuropharmacology*. 1999;38(6):735–67.
85. Parsons CG, Stöffler A, Danysz W. Memantine: a NMDA receptor antagonist that improves memory by restoration of homeostasis in the glutamatergic system—too little activation is bad, too much is even worse. *Neuropharmacology*. 2007;53(6):699–723.
86. Long NP, Kang JS, Kim HM. *Caenorhabditis elegans*: a model organism in the toxicity assessment of environmental pollutants. *Environ Sci Pollut Res*. 2023;30:39273–87. <https://doi.org/10.1007/s11356-023-25675-5>.
87. Ijomone OM, Weishaupt A-K, Michaelis V, Ijomone OK, Bornhorst J. p38- and ERK-MAPK signalling modulate developmental neurotoxicity of nickel and vanadium in the *Caenorhabditis elegans* model. *Kinases Phosphatases*. 2024;2:28–42. <https://doi.org/10.3390/kinasesphosphatases2010003>.
88. Bessa C, Maciel P, Rodrigues AJ. Using *C. elegans* to decipher the cellular and molecular mechanisms underlying neurodevelopmental disorders. *Mol Neurobiol*. 2013;48:465–89.
89. Sulston JE. Post-embryonic development in the ventral cord of *Caenorhabditis elegans*. *Philos Trans R Soc Lond B Biol Sci*. 1976;275:287–97. <https://doi.org/10.1098/rstb.1976.0084>.
90. White JG, Southgate E, Thomson JN, Brenner S. The structure of the ventral nerve cord of *Caenorhabditis elegans*. *Philos Trans R Soc Lond B Biol Sci*. 1976;275:327–48. <https://doi.org/10.1098/rstb.1976.0086>.
91. Rosini M, Simoni E, Minarini A, et al. Multi-target design strategies in the context of Alzheimer's disease: acetylcholinesterase inhibition and NMDA receptor antagonism as the driving forces. *Neurochem Res*. 2014;39:1914–23. <https://doi.org/10.1007/s11064-014-1250-1>.
92. Albert PS, Riddle DL. Developmental alterations in sensory neuroanatomy of the *Caenorhabditis elegans* dauer larva. *J Comp Neurol*. 1983;219:461–81. <https://doi.org/10.1002/cne.902190407>.
93. Yochem J. Nomarski images for learning the anatomy, with tips for mosaic analysis. *WormBook*. 2006. <https://doi.org/10.1895/wormbook.1.100>.
94. Peckol EL, Troemel ER, Bargmann CI. Sensory experience and sensory activity regulate chemosensory receptor gene expression in *Caenorhabditis elegans*. *Proc Natl Acad Sci USA*. 2001;98:11032–8. <https://doi.org/10.1073/pnas.191352498>.
95. Miyasaka T, Ding Z, Gengyo-Ando K, Oue M, Yamaguchi H, Mitani S, Ihara Y. Progressive neurodegeneration in *C. elegans* model of tauopathy. *Neurobiol Dis*. 2005;20(2):372–83.
96. Schroeder NE, Androwski RJ, Rashid A, Lee H, Lee J, Barr MM. Dauer-specific dendrite arborization in *C. elegans* is regulated by KPC1/Furin. *Curr Biol*. 2013;23:1527–35. <https://doi.org/10.1016/j.cub.2013.06.058>.

97. Raghunatha P, Vosoughi A, Kauppinen TM, Jackson MF. Microglial NMDA receptors drive pro-inflammatory responses via PARP-1/TRMP2 signaling. *Glia*. 2020;68(7):1421–34.
98. Altun ZF, Hall DH. Alimentary system: pharynx. *WormAtlas*. 2008.
99. Burr AA, Tsou WL, Ristic G, Todi SV. Using membrane-targeted green fluorescent protein to monitor neurotoxic protein-dependent degeneration of *Drosophila* eyes. *J Neurosci Res*. 2014;92(9):1100–9.
100. Momma K, Homma T, Isaka R, Sudevan S, Higashitani A. Heat-induced calcium leakage causes mitochondrial damage in *Caenorhabditis elegans* body-wall muscles. *Genetics*. 2017;206:1985–94.
101. Zheng F, Chen P, Li H, Aschner M. Drp-1-dependent mitochondrial fragmentation contributes to cobalt chloride-induced toxicity in *Caenorhabditis elegans*. *Toxicol Sci*. 2020;177(1):158. <https://doi.org/10.1093/TOXSCI/KFAA105>.
102. Kaindl AM, Degos V, Peineau S, Gouadon E, Chhor V, Loron G, Gressens P. Activation of microglial n-methyl-D-aspartate receptors triggers inflammation and neuronal cell death in the developing and mature brain. *Ann Neurol*. 2012;72(4):536–49. <https://doi.org/10.1002/ana.23626>.
103. Huang YCJ, Soukup S, Harder SB, Am J. *Physiol. Cell Physiol*. 2003;284:24–32.
104. Capella MALS, Capella RC, Valente M, Gefé AG, Lopes. *Cell Biol Toxicol*. 2007;23:413–20.
105. Zhao Y, Ye L, Liu H, Xia Q, Zhang Y, Yang X, Wang K. Vanadium compounds induced mitochondria permeability transition pore (PTP) opening related to oxidative stress. *J Inorg Biochem*. 2010;104(4):371–8.
106. Shukla RS, Padhye M, Modak SS, Ghaskadbi RR, Bhonde. *Rev Diabet Stud*. 2007;4:33–43.
107. Zhang LY, Zhang Q, Xia XM, Zhao HX, Cai DW, Li XD, Yang K, Wang ZLX. *Food chem. Toxicol*. 2008;46:2996–3002.
108. Adebisi O, Adigun K, Folarin O, Olopade J, Olayemi F. Administration of ethanolic extract of *Erythrophleum ivorense* (A Chev.) stem bark to male Wistar rats alters brain areas involved in motor coordination, behavior, and memory. *J Ethnopharmacol*. 2020;253:112650.
109. Rodríguez LR, Lapeña-Luzón T, Benetó N, Beltran-Beltran V, Pallardó FV, Gonzalez-Cabo P, Navarro JA. Therapeutic strategies targeting mitochondrial calcium signaling: a new hope for neurological diseases? *Antioxidants*. 2022;11(1):165.
110. Anderson GL, Cole RD, Williams PL. Assessing behavioral toxicity with *Caenorhabditis elegans*. *Environ Toxicol Chem Int J*. 2004;23(5):1235–40.
111. McMillen A, Chew YL. Neural mechanisms of dopamine function in learning and memory in *Caenorhabditis elegans*. *Neuronal Sign*. 2023. <https://doi.org/10.1042/NS20230057>.
112. Yu ZY, Yin DQ, Deng HP. The combinational effects between sulfonamides and metals on nematode *Caenorhabditis elegans*. *Ecotoxicol Environ Saf*. 2015;111:66–71. <https://doi.org/10.1016/j.ecoenv.2014.09.026>.
113. Chen P, Chakraborty S, Peres TV, Bowman AB, Aschner M. Manganese-induced neurotoxicity: from *C. elegans* to humans. *Toxicol Res*. 2015;4(2):191–202.
114. Chen X, Chalfie M. Modulation of *C. elegans* touch sensitivity is integrated at multiple levels. *J Neurosci*. 2014;34(19):6522–36.
115. Bwala DA, Ladagu A D. *et al*. Neurotoxic profiles of vanadium when administered at the onset of myelination in rats: the protective role of vitamin E. *Trop Veterinarian*. 2014.
116. Gatrell L, Wilkins W, Rana P, Farris M. Glucose effects on polyglutamine-induced proteotoxic stress in *Caenorhabditis elegans*. *Biochem Biophys Res Commun*. 2020. <https://doi.org/10.1016/j.bbrc.2019.11.159>.

Publisher's Note

Springer Nature remains neutral with regard to jurisdictional claims in published maps and institutional affiliations.